Research Paper

THEMED ISSUE: Mantle to Surface Dynamics during the Transition from Subduction to Collision to Tectonic Escape: Results from the Continental Dynamics–Central Anatolian Tectonics (CD-CAT) Project

GEOSPHERE

GEOSPHERE, v. 15, no. 2

https://doi.org/10.1130/GES01682.1

13 figures; 4 tables; 1 set of supplemental files

CORRESPONDENCE: goksuuslular@mu.edu.tr

CITATION: Uslular, G., and Gençalioğlu-Kuşcu, G., 2019, Mantle source heterogeneity in monogenetic basaltic systems: A case study of Eğrikuyu monogenetic field (Central Anatolia, Turkey): Geosphere, v. 15, no. 2, p. 295–323, https://doi.org/10.1130/GES01682.1.

Science Editor: Raymond M. Russo
Guest Associate Editor: Christian Teyssier

Received 20 February 2018
Revision received 6 October 2018
Accepted 15 November 2018

Published online 6 February 2019

Mantle source heterogeneity in monogenetic basaltic systems: A case study of Eğrikuyu monogenetic field (Central Anatolia, Turkey)

Göksu Uslular and Gonca Gençalioğlu-Kuşcu

Department of Geological Engineering, Muğla Sıtkı Koçman University, Muğla TR48000, Turkey

ABSTRACT

The Eğrikuyu monogenetic field is located in the southwestern part of the Central Anatolian volcanic province and includes numerous scoria cones and related lava flows, as well as a few maars. Eğrikuyu monogenetic field basalts are mainly olivine-nepheline (Ol-Nph) normative, with higher MgO (7.9–11.5 wt%) and Ni (up to 226 ppm) contents compared to other Central Anatolian volcanic province basalts. Enrichment in large ion lithophile elements compared to high field strength elements and depletions in Nb, Ta, P, and Ti in the multi-element diagrams are typical trace-element characteristics of all Central Anatolian volcanic province basalts. Mineral, trace element, and isotope compositions of Eğrikuyu monogenetic field basalts revealed the necessity of at least two distinct and variously enriched components responsible for their formation. Decompressional melting of metasomatized subcontinental lithospheric mantle (enriched mid-ocean-ridge basalt–like), with or without the contribution of upwelling deep asthenospheric melt (oceanic-island basalt–like), may explain the geochemical characteristics of all Central Anatolian volcanic province basalts. The lower $^{207}Pb/^{204}Pb$ ratios and some distinct clinopyroxene compositions (titaniferous augite and Fe-rich diopside) in Eğrikuyu monogenetic field basalts are indicators for the presence of upwelling asthenosphere, which is also evident in the low-seismic-velocity anomalies and Cyprian slab tear that underlie the field. The Eğrikuyu monogenetic field is a good example of mantle source heterogeneity in a monogenetic basaltic field and therefore constitutes a suitable region within the Central Anatolian volcanic province where different mantle source components can be traced.

INTRODUCTION

Monogenetic basaltic fields are spectacular volcanic landscapes that consist of numerous scoria (or cinder) cones, maars, and related lava flows (e.g., Wood, 1980; Connor and Conway, 2000; Valentine and Gregg, 2008; Kereszturi and Németh, 2012; Németh and Kereszturi, 2015; Smith and Németh, 2017), and they occur in different tectonic settings, including subduction zones (e.g., Trans-Mexican volcanic belt; Luhr et al., 1989) and extensional environments (e.g., Auckland volcanic field; McGee et al., 2013). Source heterogeneity, either in an individual monogenetic volcano (sensu lato) or the entire monogenetic basaltic field with respect to the geographical distribution and size of the eruptive centers, and the temporal evolution of monogenetic fields have been recently reported from different parts of the world (e.g., Shaw et al., 2003; Strong and Wolff, 2003; Brenna et al., 2010; McGee et al., 2013; Rasoazanamparany et al., 2015; Báez et al., 2017). Possible mechanisms proposed to explain this variation are various degrees of crystallization or melting, crystal-melt interaction, multiple components of the mantle source, and ascent dynamics (e.g., Kereszturi and Németh, 2012; McGee et al., 2013; Smith and Németh, 2017). Therefore, investigation of primitive basalts in monogenetic fields will provide new insight into the evolution of basaltic melt from the mantle, and monogenetic fields should be analyzed systematically in terms of their morphological, petrological, and volcanological processes (McGee et al., 2013).

Alkalinity is an important parameter of basaltic volcanic fields that helps in understanding possible mantle sources. Melts formed at high pressures have a deficiency in SiO_2 compared to those formed at low pressures (e.g., Hirose and Kushiro, 1993). Therefore, SiO_2 undersaturation (e.g., nepheline [Nph] normative) in many alkali basaltic rocks is believed to represent magmas formed by partial melting at greater depths (i.e., asthenosphere) than subalkali magmas (Gill, 2010, and references therein). The transition from calc-alkaline (i.e., subduction-related) to alkaline (i.e., within-plate–like) magmatism is a common process in postcollisional settings (e.g., circum-Mediterranean region; Lustrino and Wilson, 2007). Na-alkaline affinity with oceanic-island basalt (OIB)–like trace-element compositions is one of the main indicators of alkaline magmatism in such regions. Various hypotheses have been proposed for the origin of Na-alkalinity in basaltic magmas (e.g., recycled lithologies in the asthenosphere), but the melting of metasomatized lithosphere with a contribution from low-degree asthenospheric melts is the most suitable model, especially for explaining the similar major- and trace-element compositions of both K- and Na-alkaline magmas in continental settings (Pilet, 2015, and references therein).

The Central Anatolian volcanic province is a SW-NE–trending volcanic belt limited by strike-slip fault systems (i.e., Tuz Gölü and Ecemiş; Toprak, 1998), and it is thought to have evolved in an extensional or transtensional environment since Late Cretaceous time (Genç and Yürür, 2010) in between extensional western Anatolia and compressional eastern Anatolia (Fig. 1A). Plateau-like topography (~1 km elevation), low seismic (Pn and shear) velocities in shallow depths (15–25 km; e.g., Gans et al., 2009; Mutlu and Karabulut,

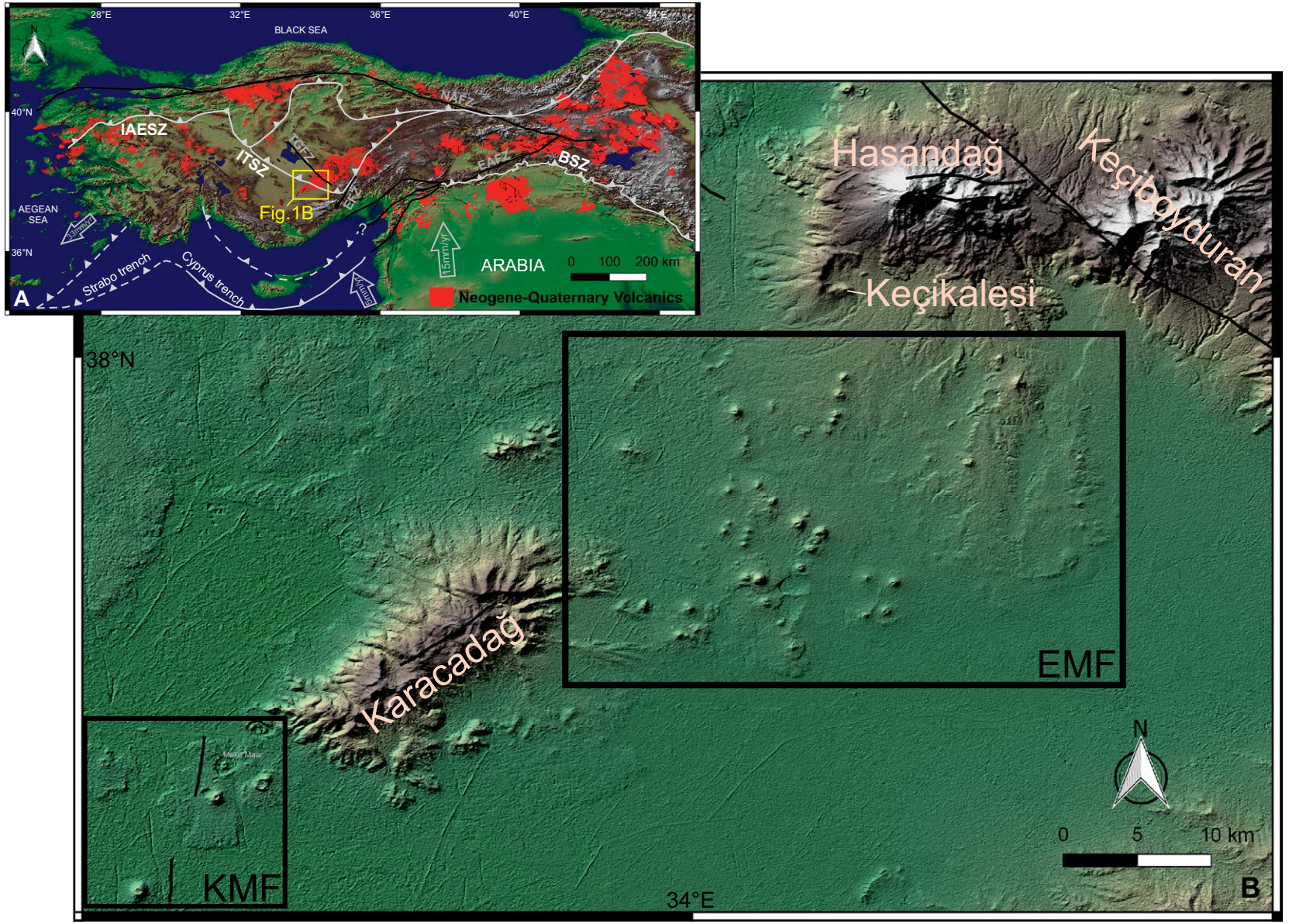

Figure 1. (A) Distribution of Neogene–Quaternary volcanics throughout Anatolia (compiled from Şenel, 2002, geological map) displayed on a colored Shuttle Radar Tomography Mission (SRTM) image. The main tectonic structures and suture zones are from Okay and Tüysüz (1999). Blank arrows indicate the plate motions with respect to the Eurasian plate (Reilinger et al., 2006). IAESZ—İzmir-Ankara-Erzincan suture zone; ITSZ—Inner Tauride suture zone; BSZ—Bitlis suture zone; NAFZ—North Anatolian fault zone; EAFZ—Eastern Anatolian fault zone; TGFZ—Tuz Gölü fault zone; EFZ—Ecemiş fault zone. (B) Colored digital elevation model (DEM) image (30 m × 30 m Advanced Spaceborne Thermal Emission and Reflection Radiometer [ASTER] Global Digital Elevation Map [GDEM]) showing polygenetic volcanoes and monogenetic fields in the southern part of Central Anatolian volcanic province. EMF—Eğrikuyu monogenetic field; KMF—Karapınar monogenetic field.

2011; Abgarmi et al., 2017; Delph et al., 2017; Reid et al., 2017), and various Curie point depths (2–22 km; Ateş et al., 2005) and crustal thicknesses (Uluocak et al., 2016; Abgarmi et al., 2017) are observed throughout central Anatolia. The different episodes of uplift associated with asthenospheric upwelling (Cosentino et al., 2012) or isostatic adjustments (Schildgen et al., 2012; Abgarmi et al., 2017) after slab break-off or drip-tectonism (Göğüş et al., 2017) are some of the most important geodynamic processes in the Neogene–Quaternary evolution of central Anatolia. The ~25,000 km^2 Central Anatolian volcanic province is defined by widespread ignimbrite eruptions (ca. 9.1–2.5 Ma), Miocene–Pliocene polygenetic volcanoes (e.g., Tekkedağ, Develidağ), Quaternary stratovolcanoes (Hasandağ and Erciyes), and more than 800 monogenetic volcanoes (mainly scoria cones with subordinate maars and lava domes; Toprak, 1998). There is still no consensus on the Neogene–Quaternary petrological evolution of the Central Anatolian volcanic province basalts, which have strong arc-like trace-element patterns (depletion in high field strength elements [HFSEs]) in multi-element diagrams (e.g., Deniel et al., 1998; Kürkçüoğlu et al., 1998; Alıcı-Şen et al., 2004; Gençalioğlu-Kuşcu and Geneli, 2010; Gençalioğlu-Kuşcu, 2011; Reid et al., 2017), unlike their mildly Na-alkaline affinity (e.g., Aydin et al., 2014; Uslular, 2016). Despite some questionable attempts at claiming "OIB-like" trace-element compositions, especially for Quaternary Central Anatolian volcanics (Aydin, 2008; Güçtekin and Köprübaşı, 2009), it is almost impossible to reveal a clear transition from orogenic (i.e., subduction-related) to anorogenic (within-plate–like) volcanism in the Central Anatolian volcanic province using whole-rock geochemistry alone. However, various source components have been recently proposed for the petrological evolution of volcanics in the Central Anatolian volcanic province, where the presence of OIB-like affinity is fairly limited and only revealed in some trace-element ratios (e.g., Reid et al., 2017). This subject is certainly open to discussion and has been tackled in detail throughout this paper.

Some studies on the Central Anatolian volcanic province are mainly focused on the monogenetic fields (Keller, 1974; Gençalioğlu-Kuşcu, 2011), while most studies (Ercan et al., 1992; Notsu et al., 1995; Alıcı-Şen et al., 2004; Gençalioğlu-Kuşcu and Geneli, 2010; Aydin et al., 2014; Reid et al., 2017) concern the source and possible mechanism that triggered the extensive volcanism within the Central Anatolian volcanic province in general. The Eğrikuyu monogenetic field is one of the basaltic monogenetic fields in the Central Anatolian volcanic province with numerous scoria cones and related basaltic lava flows, and at least six maars (Kutören, Obruk, Develiini, Çayankışlası, Karafatma, and Leşkeri; Fig. 2; Uslular et al., 2015, and references therein). Petrological studies have revealed that despite their Na-alkaline affinity, the mildly alkaline Eğrikuyu monogenetic field basalts have typical arc-like trace-element compositions, and they could be derived from enriched subcontinental lithosphere with or without a contribution from deep asthenosphere that may have risen through a slab tear (Ercan et al., 1992; Notsu et al., 1995; Alıcı-Şen et al., 2004; Uslular, 2016; Reid et al., 2017).

This paper reports a detailed petrological investigation of the Eğrikuyu monogenetic field basalts using a monogenetic volcanism perspective that included mineral, major and trace element, and isotope geochemistry. We emphasize the geochemical diversity observed in this small monogenetic basaltic field that was possibly generated by different degrees of melting and/or various mantle source components with minor contributions of mafic mineral fractionation and crustal contamination.

CENTRAL ANATOLIAN VOLCANIC PROVINCE: A MONOGENETIC OVERVIEW

Some segments of the northern Neo-Tethys ocean were closed during the middle-to-late Paleogene collision between the Anatolide-Tauride and Kırşehir blocks along the İzmir-Ankara-Erzincan suture zone to the north, and the Inner Tauride suture zone to the south (e.g., Görür et al., 1984). Subsequently, the collision of the Afro-Arabian and Eurasian plates along the Bitlis suture zone (Fig. 1A) closed the southern branch of Neo-Tethys ocean in the early Miocene (Okay et al., 2010). The interplay of collisional events and subsequent processes (i.e., extensional tectonism after at least the late Miocene, with localized strike-slip faults; e.g., Koçyiğit and Beyhan, 1998; Genç and Yürür, 2010; Özsayın et al., 2013) likely controlled widespread volcanism throughout the Central Anatolian volcanic province. In addition, uplift and geodynamic processes, such as delamination and slab break-off (Bartol and Govers, 2014), associated with ca. 15 Ma volcanism in Eastern Anatolia point to coeval processes and related origins for both the Eastern and Central Anatolian volcanic provinces. However, recent geophysical (Abgarmi et al., 2017; Delph et al., 2017), geodynamic modeling (Göğüş et al., 2017), and petrological (Reid et al., 2017) studies revealed difficulties in calling for single-slab delamination along Central and Eastern Anatolia (Bartol and Govers, 2014). The causes of different episodes of uplift that have varied geographically throughout Central Anatolia (i.e., different in northern, central, and southern parts; Schildgen et al., 2014) have been recently discussed in the literature (Abgarmi et al., 2017; Delph et al., 2017; Göğüş et al., 2017). Uplift in the central and southern parts of Central Anatolia is especially important in terms of volcanism, but whether uplift was caused by asthenospheric upwelling (Genç and Yürür, 2010; Cosentino et al., 2012), topographic response after slab break-off (Schildgen et al., 2012, 2014; Abgarmi et al., 2017), or alternatively after lithosphere dripping (Göğüş et al., 2017) is still debatable. Therefore, we believe that further investigation, especially regarding the relationship between uplift and widespread volcanism in the Central Anatolian volcanic province, will provide new insight into the geodynamic evolution of Central Anatolia.

The recently proposed geodynamic models used to explain widespread Central Anatolian volcanism can be summarized as follows (Bartol and Govers, 2014; Schildgen et al., 2014; Reid et al., 2017; Abgarmi et al., 2017; Delph et al., 2017; Schleiffarth et al., 2018): (1) In the mid-late Miocene, rollback of the delaminating Anatolide-Tauride and Kırşehir mantle lithosphere gave rise to asthenospheric upwelling and interaction with the crust, initiating widespread explosive ignimbritic volcanism. (2) Continued slab rollback caused SW mi-

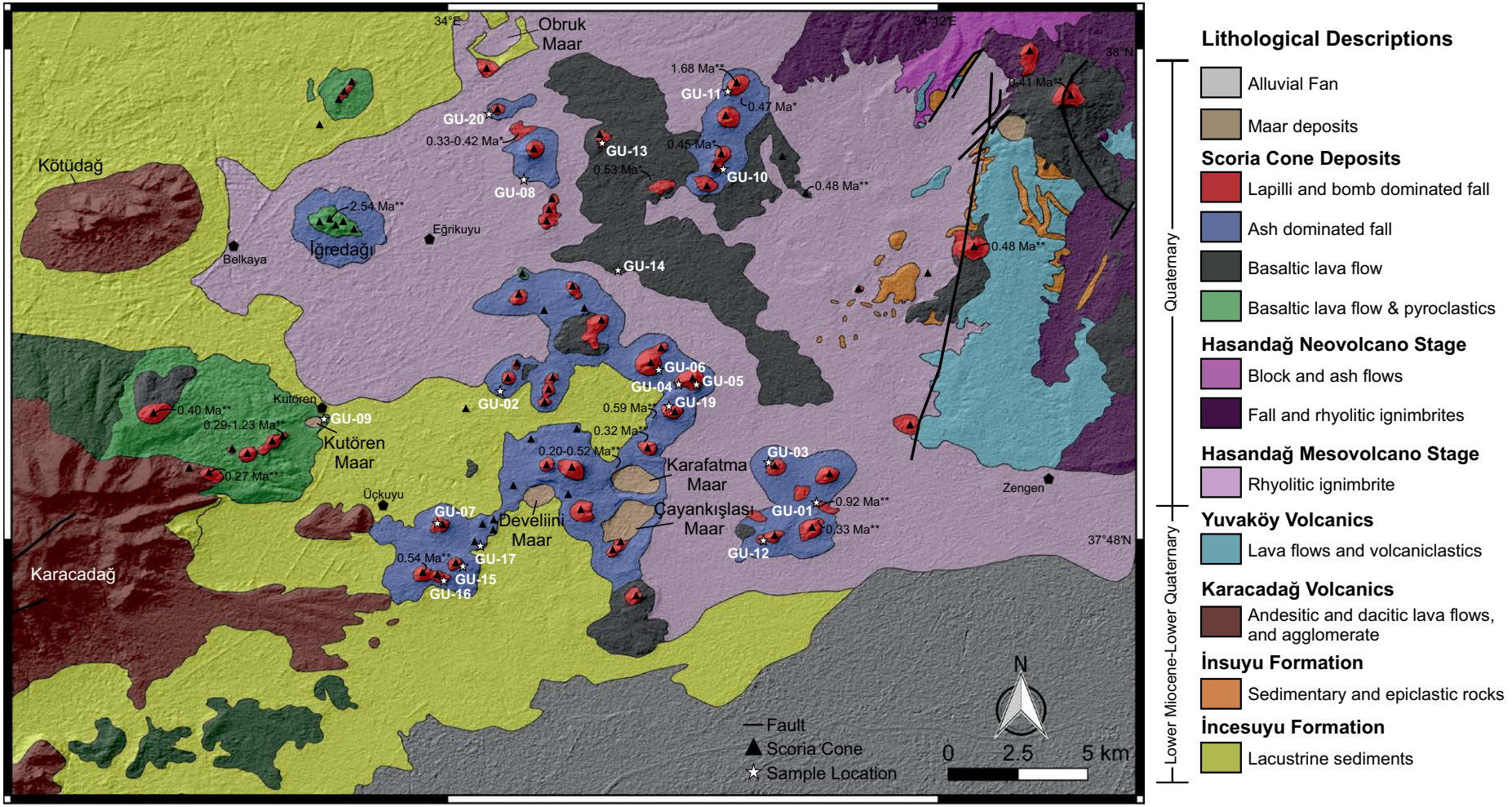

Figure 2. Simplified geological map of the Eğrikuyu monogenetic field (modified from Şenel, 2005, and Ulu, 2009, geological maps) displaying sample locations and age data from the literature (*Notsu et al., 1995; **Reid et al., 2017).

gration of volcanism, and subsequent slab break-off in the latest Miocene led to the initiation of uplift that accelerated in the late Pliocene–early Pleistocene owing to crustal rebound. This model is mainly based on geophysical interpretations, but petrological characteristics of volcanics, especially in the southernmost part of the Central Anatolian volcanic province, also support the contribution of upwelling asthenosphere (Reid et al., 2017). Delamination of the Anatolide-Tauride and Kırşehir mantle lithosphere around mid-Miocene time was also suggested by Kadıoğlu and Dilek (2010). However, the late Miocene to recent processes beneath Central Anatolia are especially crucial for a better understanding of Central Anatolian volcanic province volcanism.

Monogenetic volcanoes display spectacular landscapes throughout the Central Anatolian volcanic province, either as scattered cones on the flanks of stratovolcanoes (e.g., Hasandağ, Erciyes, Keçiboyduran) or as monogenetic fields (e.g., Eğrikuyu, Karapınar; Fig. 1B). Volcanic fields in the Central Anatolian volcanic province that include monogenetic volcanoes are briefly explained as follows:

Hasandağ-Karacadağ Volcanic Field

Hasandağ-Karacadağ volcanic field consists of numerous scoria and parasitic cones, several lava domes, and a few maars related to different evolutionary stages (paleovolcano, mesovolcano, and neovolcano) of the Hasandağ stratovolcano (Aydar et al., 1995; Aydar and Gourgaud, 1998; Deniel et al., 1998). Different types of monogenetic volcanoes (i.e., scoria cones, lava domes) formed randomly during the evolution of Hasandağ, and therefore there is no clear temporal evolution within these edifices based on available radiometric ages (e.g., Aydar and Gourgaud, 1998; Reid et al., 2017). These cones are mainly clustered in the southern (NE of Eğrikuyu monogenetic field) and northwestern (around Karataş village) parts of the Hasandağ (Fig. 1B). The cones around Karataş are elongated in a NW-SE direction (parallel to the Tuz Gölü fault zone), whereas those in the southern part have generally N-S or NE-SW (parallel to the Ecemiş fault zone) trends. While scoria cones are mainly basaltic, lava domes are more felsic in composition (Aydar et al., 1995; Notsu et al., 1995; Deniel et al., 1998). Reid et al. (2017) recently published Ar-Ar ages (1.75–0.37 Ma) for some of the basaltic scoria cones and related lava flows in the southern part of Hasandağ and Karataş field (Table 1). Karacadağ volcano is an andesitic polygenetic volcano of Miocene–Pliocene age (5.98–4.68 Ma; Platzman et al., 1998) in the area. Karapınar monogenetic field and Eğrikuyu monogenetic field are individual monogenetic fields of Quaternary age (Table 1) to the southwest of Karacadağ and Hasandağ, respectively. Therefore, they are considered as distinct clusters in this paper.

Karapınar Monogenetic Field

Karapınar monogenetic field is located at the southwestern tip of the Central Anatolian volcanic province, close to the Karacadağ stratovolcano (Fig. 1B), and it consists of basaltic scoria cones and maars of Pleistocene age (Table 1; Keller, 1974; Ercan et al., 1992; Notsu et al., 1995; Alıcı-Şen et al., 2004; Reid et al., 2017). The main alignment of the monogenetic volcanoes in the Karapınar monogenetic field is NE-SW, consistent with the elongation of the Karacadağ stratovolcano (Toprak, 1998). Meke maar is a spectacular monogenetic edifice in the Karapınar monogenetic field that includes a scoria cone in the center (Fig. 1B; Keller, 1974). Considering the available age data, there is no clear transition between magmatic and phreatomagmatic eruptions in the region. In Pleistocene time, the southwestern part of the Central Anatolian volcanic province close to the Karapınar monogenetic field was occupied by pluvial lakes with high water levels (e.g., Bayer-Altın et al., 2015, and references therein). In addition, during that time, Central Anatolia is thought to have been uplifted due to Cyprian slab break-off (e.g., Schildgen et al., 2014). All these resulted in variable hydrogeological conditions in both the Karapınar monogenetic field and the Central Anatolian volcanic province, where water probably was supplied by a combination of porous media and fracture-controlled aquifers, similar to the Tihany Maar volcanic complex in the Pannonian Basin (Németh et al., 2001). However, the link between hydrogeological conditions and the formation of various types of monogenetic volcanoes in the Central Anatolian volcanic province still needs to be resolved.

Niğde Volcanic Field

Niğde volcanic field includes three stratovolcanoes, namely, Melendiz, Keçiboyduran, and Tepeköy, along with numerous monogenetic volcanoes (mainly scoria cones and a few domes). There is a wide spectrum in the composition of the volcanics, from basalt to rhyolite (Batum, 1978; Aydin, 2008; Gençalioğlu-Kuşcu and Geneli, 2010; Aydin et al., 2014). The monogenetic volcanoes are clustered in three main groups, similar to those to the northwest of Keçiboyduran volcano, south of Melendiz volcano, and northwest of Tepeköy volcano (Toprak, 1998). The monogenetic volcanoes in the first two clusters (e.g., 0.65–0.22 Ma for the scoria cones of Keçiboyduran; Aydin et al., 2014) are partly buried by the recent ash deposits of the Hasandağ volcano in the north and recent alluvial deposits in the south. Göllüdağ rhyolitic dome complex (Batum, 1978) is located north of the Tepeköy stratovolcano, with a surface area of almost 90 km^2 (Toprak, 1998). It is composed of rhyolitic and rhyodacitic lava flows and related obsidian and perlitic rocks (Batum, 1978; Aydin et al., 2014). Recent age data (U-Pb on zircon) reveal that rhyolitic lavas and pumice clasts from the Göllüdağ dome are 1.08 Ma and 0.89 Ma, respectively (Aydin et al., 2014; see also Table 1 herein).

Acıgöl Volcanic Field

Acıgöl volcanic field is represented by widespread Pleistocene pyroclastic fallout and flow deposits related to the Acıgöl caldera (~6 × 5 km), and it is divided into two groups, the Lower Acıgöl Tuff and the Upper Acıgöl Tuff (Druitt et al., 1995). In addition, there are two clusters of rhyolitic domes, older domes to the east (e.g., Kocadağ, Boğazköy), and N-S–oriented younger domes with well-preserved tuff rings to the west (e.g., Karnıyarık, Kuzey, Güneydağ, Korudağ; Schmitt et al., 2011). The first group of domes is exposed along a N-S–oriented scarp resulting from downfaulting during Upper Acıgöl Tuff eruption (Druitt et al., 1995). However, the caldera margins are absent in the west and the north, and they predate the eruption of Upper Acıgöl Tuff in the south (Druitt et al., 1995), probably resulting from a fissure eruption or trapdoor caldera system with a N-S–oriented hinge zone (Türkecan et al., 2004). Acıgöl volcanic field also displays a great variety of monogenetic volcanoes (i.e., scoria cones, maars, lava domes, and tuff cones), especially in terms of different eruption styles and compositions (Toprak, 1998). Basaltic scoria cones and rhyolitic lava domes are the dominant monogenetic volcanoes in the region. Maars (e.g., Acıgöl) represent the youngest volcanic activity (20.3 ka; ^{14}C and U-Th/He methods; Kuzucuoğlu et al., 1998; Schmitt et al., 2011; see also Table 1 herein) in the area and spatially coincide with the younger domes.

TABLE 1. REVIEW OF QUATERNARY MONOGENETIC FIELDS IN THE CENTRAL ANATOLIAN VOLCANIC PROVINCE

Monogenetic field	Edifice	Composition	Alignment	Approx. age (Ma)	Method
KMF	Lava dome Scoria cone Maar	Basaltic Trachybasaltic Andesitic	NE-SW	0.16–0.28[f] 0.29–0.50[e]	K-Ar Ar-Ar
EMF	Scoria cone Maar	Basaltic Trachybasaltic	NE-SW N-S NW-SE	0.07–0.80[f] 0.21–2.57[e]	K-Ar Ar-Ar
HKVF	Lava dome Scoria cone Maar	Basaltic to rhyolitic	NE-SW N-S NW-SE	0.01–0.03[c] 0.02–0.54[f] 0.37–1.75[e]	(U-Th)/He K-Ar Ar-Ar
NVF	Lava dome Scoria cone	Basaltic to rhyolitic	NW-SE	0.22–0.65[d] 0.89–1.08[d]	Ar-Ar U-Pb
AVF	Lava dome Scoria cone Maar	Basaltic to rhyolitic	N-S NE-SW NW-SE	0.02–0.19[b]	(U-Th)/He
EVF	Lava dome Scoria cone Maar	Basaltic to rhyolitic	–	0.13–0.35[a] 0.01–1.70[f]	K-Ar K-Ar

Note: Age data are restricted to those published in the last decade: a—Gençalioğlu-Kuşcu (2011); b—Schmitt et al. (2011); c—Schmitt et al. (2014); d—Aydin et al. (2014); e—Reid et al. (2017); f—Doğan-Külahcı et al. (2018). For a more comprehensive age compilation, please see Türkecan et al. (2004). Alignments are from Toprak (1998). KMF—Karapınar monogenetic field; EMF—Eğrikuyu monogenetic field; HKVF—Hasandağ-Karacadağ volcanic field; NVF—Niğde volcanic field; AVF— Acıgöl volcanic field; EVF— Erciyes volcanic field.

Erciyes Volcanic Field

Erciyes volcanic field is a unique area marked by the occurrence of hundreds of parasitic cones located on the flanks of the Erciyes stratovolcano along the radial fissures of its central vent (Toprak, 1998). The new Erciyes stage (Kürkçüoğlu et al., 1998; Şen et al., 2003) also includes rhyodacitic domes (e.g., Dikkartın Dağ; Şen et al., 2002), a basaltic-andesitic maar volcano (Cora maar; Gençalioğlu-Kuşcu et al., 2007; Gençalioğlu-Kuşcu, 2011), and numerous basaltic parasitic scoria cones on the flank of the volcano (Toprak, 1998; Şen et al., 2003). Based on published radiogenic ages, monogenetic volcanism in the Erciyes volcanic field lasted between 2.56 and 0.88 Ma (Notsu et al., 1995; Şen et al., 2003; Gençalioğlu-Kuşcu, 2011; Doğan-Külahçı et al., 2018; see also Table 1 herein).

Eğrikuyu Monogenetic Field

Eğrikuyu monogenetic field is a Quaternary basaltic intraplate monogenetic field represented by more than 100 scoria cones and a few maar volcanoes (e.g., Obruk, Kutören) within an area of 900 km^2 located in the southwestern sector of the Central Anatolian volcanic province (Figs. 1B and 2). Toprak (1998) analyzed the relationship between tectonic lineaments and the spatial distribution of scoria cones and suggested that the clustering of volcanic centers in the area follows two dominant trends. Arcasoy (2001) also studied the clustering and alignments of point-like features (i.e., volcanic centers) and revealed the same dominant trends within the Eğrikuyu monogenetic field. These trends are NE-SW in the west (i.e., NE of Karacadağ stratovolcano) and N-S to NW-SE toward the east (i.e., between Karacadağ and the south of Hasandağ; Fig. 2; Toprak, 1998). As in the case of the other monogenetic fields in the Central Anatolian volcanic province, clustering directly indicates that the occurrence of monogenetic volcanoes in the Eğrikuyu monogenetic field was directly controlled by the main fault systems in the region (Figs. 1B and 2). For instance, the NE-SW trend of scoria cones to the NE of Karacadağ is a direct indication of a fault buried by the accumulation of younger sediments, which also gave rise to the formation of Karacadağ stratovolcano parallel to the Central Anatolian volcanic province long axis (Fig. 2; Toprak, 1998). However, the scoria cones clustered further to the northeast (between Karacadağ and Hasandağ, and south of Hasandağ) are related to the southern extension of the Tuz Gölü fault zone, which changes direction from NW-SE to N-S (Toprak, 1998). Additionally, some of the cones (e.g., Leşkeri Hill) are cut by faults within the Tuz Gölü fault zone, indicating contemporaneous activity of faulting and volcanism (Fig. 2; Toprak, 1998).

Most of the scoria cones within the Eğrikuyu monogenetic field are breached-type features (Uslular et al., 2015), due to possible flow emittance, flank collapse, and basal inclination (e.g., Németh et al., 2011). Detailed information on the morphological features of the cones in the Eğrikuyu monogenetic field can be found in Uslular et al. (2015). The interplay of eruptive styles from "dry" magmatic to "wet" phreatomagmatic processes is clearly observed in the Eğrikuyu monogenetic field (Fig. 2). Hydrological conditions in

the Eğrikuyu monogenetic field during the Quaternary were variable, similar to other regions in the Central Anatolian volcanic province (especially Karapınar monogenetic field), owing to regional uplift and climatic changes (e.g., Schildgen et al., 2014; Bayer-Altın et al., 2015, and references therein). Considering the fact that maar volcanoes within the Eğrikuyu monogenetic field have not been studied in detail, the relative age relationships between maars and scoria cones are not clear.

Lava flows are vesicular, dense, and olivine-phyric, displaying typical 'a'ā type lava morphology with blocky outcrops (Figs. 3A and 3B). In addition, carbonate minerals filled the vesicles of lava flows, especially those sampled in the western part of the Eğrikuyu monogenetic field. Lapilli- and bomb-size basaltic scoria are the main pyroclastic deposits of the scoria cones in the region (Figs. 3C and 3D). Some of the scoria cones have ash- to lapilli-sized tephra layers at their lower parts. These slightly stratified tephra layers are related to either former maar formation or initial phreatomagmatic activity during the formation of scoria cones (e.g., Kereszturi and Németh, 2012). Maars in the Eğrikuyu monogenetic field display typical base surge deposits with lapilli-sized scoria-fall deposits (Figs. 3E and 3F). Basaltic scoria cones and associated lava flows have been studied in terms of their petrological evolution (Ercan et al., 1992; Notsu et al., 1995; Reid et al., 2017). In general, volcanics in the Eğrikuyu monogenetic field are high-Mg basalts with a typical subduction signature in multi-element diagrams. Reid et al. (2017) recently studied the petrological evolution of volcanic rocks in the Eğrikuyu monogenetic field and surrounding the Hasandağ stratovolcano, and they published Ar-Ar ages (2.57–0.21 Ma) that are mainly clustered around 0.4 Ma, similar to those proposed by Notsu et al. (1995).

SAMPLING AND METHODOLOGY

Fresh fallout deposits and lava flows of scoria cones and maars for thin section and whole-rock analysis were collected in and around the Eğrikuyu monogenetic field. Most of the samples are lava flows associated with scoria cones, because eruptive products of scoria cones exposed on their surfaces are generally altered, and quarried scoria cones are not always available for collecting fresh samples. In total, 25 thin sections were prepared at Vommak Mechanical Engineering Ind. Trade., Co., Ltd. (Ankara, Turkey). Of those, 20 relatively fresh samples were selected for geochemical analyses that were performed in the ACME Analytical Laboratories Ltd. (Canada) using an inductively coupled plasma–atomic emission spectrometer (ICP-OES) for major elements and inductively coupled plasma–mass spectrometer (ICP-MS) for trace and rare earth elements (REEs). The standards (STD SO-18) used for the geochemical analysis of all Eğrikuyu monogenetic field basalts are reported in the Supplemental File[1].

After performing the CIPW norm calculations, Eğrikuyu monogenetic field basalts were divided into two main groups based on the classification of Thompson (1984). The majority of the samples are olivine-nepheline (Ol-Nph) normative alkali basalts (AB), and only two samples are olivine-hypersthene (Ol-Hyp) normative transitional basalts (TB) (mineral abbreviations throughout the paper are from Whitney and Evans, 2010). Therefore, samples for further analysis, such as mineral and isotope chemistry, were selected depending on this classification. In addition, this nomenclature is also used throughout the paper for geochemical interpretations. The compositions of olivine (Ol), clinopyroxene (Cpx), plagioclase (Pl), and some Fe-Ti oxides were analyzed in 10 polished sections using an electron microprobe (JEOL JXA 8900 R) at the University of Minnesota (USA) and University of Göttingen (Germany). Detailed descriptions for the analysis are given in the Supplemental File (footnote 1). The Sr, Nd, and Pb isotope analyses of 10 samples were performed at the Radiogenic Isotope Laboratory of Central Laboratory, Middle East Technical University, Ankara, Turkey. Detailed descriptions of analytical procedures for Sr, Nd, and Pb isotopes, explained by Köksal et al. (2017), are given in the Supplemental File (footnote 1).

RESULTS AND DISCUSSION

Petrography

In total, 25 thin sections from fallout and flow deposits of scoria cones and maars within the Eğrikuyu monogenetic field were examined under the microscope in terms of mineral contents and textural characteristics. The main mineral assemblages of the lava flows are Pl, Ol, Cpx, and oxides found as phenocrysts and microphenocrysts, and microlites. The only difference in these rocks is the relative proportions of the mineral phases (i.e., lava flows have a higher amount of Pl compared to fallout deposits; cf. Figs. 4A and 4D). The samples display porphyritic or seriate texture with the microphenocrysts or microlites and interstitial glass (Fig. 4B). The abundance of Ol and Cpx microphenocrysts and microlites in AB samples increases with an alkaline affinity (sample GU-16 has the highest normative Nph content; Fig. 4C). Lava flows mainly display trachytic texture (Fig. 4D), with some exceptions showing pilotaxitic texture (Fig. 4E), whereas all the fallout samples are pilotaxitic (Figs. 4A and 4E). Some vesicles in scoria samples are filled by secondary minerals (generally calcite). Cumulates of Cpx and Ol microphenocrysts are especially observed in fallout deposits (Fig. 4F). Subidiomorphic plagioclase microphenocrysts in some rocks display zoning (Fig. 4B). There are many indications of disequilibrium between minerals and melt (or rapid cooling of magma) in the Eğrikuyu monogenetic field basalts, such as skeletal Ol and Cpx minerals, zoning, especially in Ol, and sector (or hourglass) zoning in Cpx (Figs. 4A, 4D, and 4E).

Rock Classification

To quantify the degree of silica saturation in the Eğrikuyu monogenetic field basalts in comparison to other Anatolian basalts, major-element analyses of the rocks were used to calculate the CIPW normative mineralogy (Johannsen, 1931). However, it may be unreliable to calculate the normative

ANALYTICAL PROCEDURES

Electron Micro-Probe Analysis (EMPA)

EMPA were performed on EMF basalts in two different laboratories. Therefore, analysis procedures will be explained for each as follows.

Procedures in the laboratories at University of Minnesota (USA)

Compositional analyses were acquired on an electron microprobe (JEOL JXA-8900R) equipped with 5 tunable wavelength dispersive spectrometers. Operating conditions were 40 degrees takeoff angle, and a beam energy of 15 keV. The beam current was 20 nA, and the beam diameter was 10μm. Elements were acquired using analyzing crystals LiFH for Mn, Fe, PETJ for Ca, Ti, Cr, K, and TAP for Si, Al, Mg, Na. The standards were Anorthite, NMNH 137041 for Al, Ca, Chromite, NMNH 117075 for Cr, Hornblende (Kakanui), NMNH 143965 for Mg, Ilmenite, NMNH 96189 for Ti, Fe, Microcline (Asbestos) for K, Mn-olivine, GRR392, Mn_2SiO_4 for Mn, and Albite, Taylor, $NaAlSi_3O_8$ for Si, Na. The counting time was 20 seconds for all elements. The off peak counting time was 20 seconds for all elements. The off peak correction method was Linear for all elements. Unknown and standard intensities were corrected for deadtime. Standard intensities were corrected for standard drift over time. Area Peak Factors (APF) were utilized to correct x-ray intensities for wavelength peak shift and/or shape changes for compound compositions by summing binary APF values (see Bastin and Heijligers, 1986)

Results are the average of 4 points and detection limits ranged from 0.011 weight percent for Mg to 0.013 weight percent for Si to 0.018 weight percent for Ca to 0.028 weight percent for Cr to 0.035 weight percent for Fe. Analytical sensitivity (at the 99% confidence level) ranged from 0.270 percent relative for Mg to 0.285 percent relative for Si to 10.200 percent relative for Mn to 75.459 percent relative for Ti to 126.898 percent relative for K. Oxygen was calculated by cation

[1]Supplemental Material. Supplemental File: Analytical procedures. Supplemental Data: Whole data set of mineral chemistry analyses by EMPA. Please visit https://doi.org/10.1130/GES01682.S1 or access the full-text article on www.gsapubs.org to view the Supplemental Material.

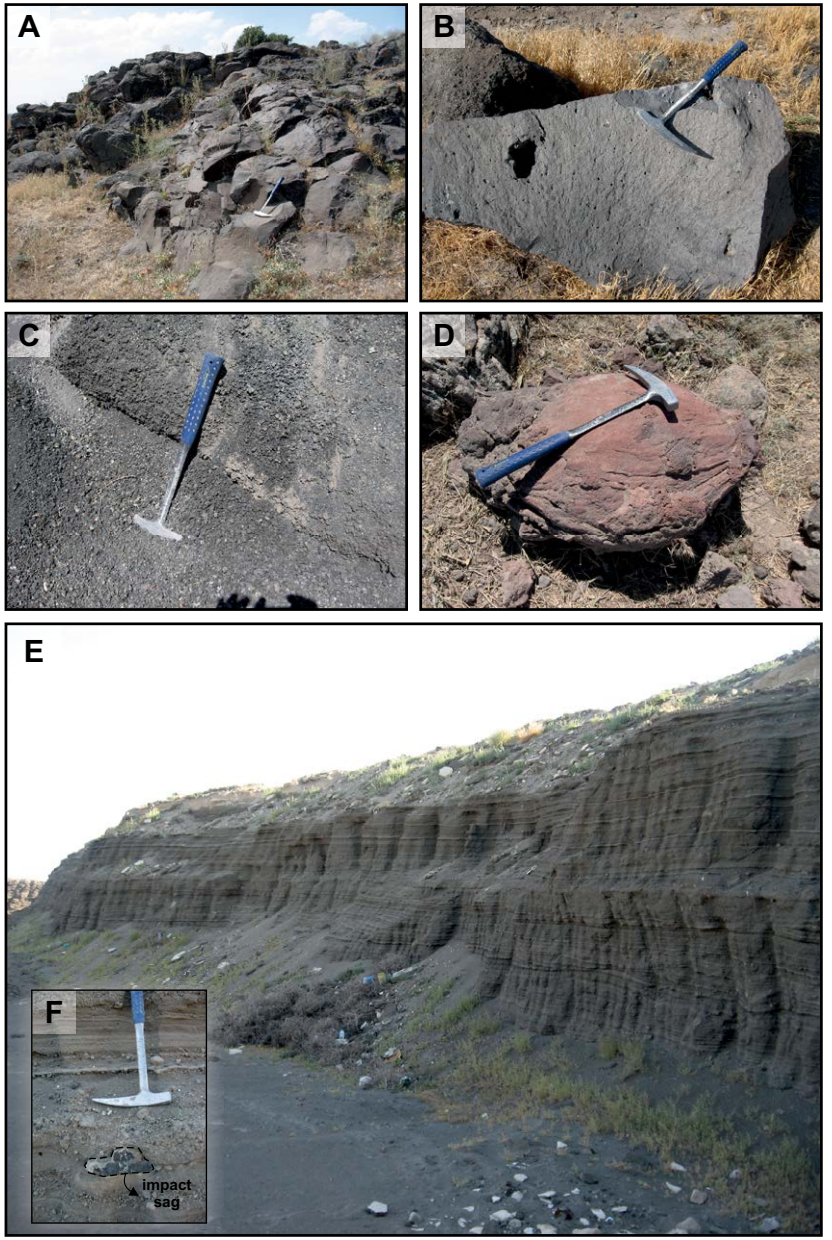

Figure 3. (A) Outcrop of a blocky-lava flow. (B) Close-up view of A. (C) Scoria-lapilli-fall deposit. (D) Spindle-shaped bomb. (E) Kutören maar rim, including stratified tephra layers. (F) Close-up view of impact sag and stratified ash-lapilli–sized tephra layer in Kutören maar (hammer is 41 cm long).

mineralogy of rocks that are derived from the continental lithosphere where the interaction with silica-rich wall rocks is inevitable, because this decreases the normative nepheline (Nph) or increases the normative hypersthene (Hyp) contents (e.g., DePaolo and Daley, 2000). Therefore, normative classification of relatively evolved samples might result in misleading interpretations and should be used considering the effects of crustal assimilation processes (e.g., DePaolo and Daley, 2000). On the other hand, the loss on ignition (LOI) value is an important indicator for understanding the alteration effects or analytical problems. In order to minimize such effects, samples with less than ~3 wt% LOI were considered for the interpretation of both Eğrikuyu monogenetic field (0.3–2.4 wt%) and Anatolian basalts (0–3 wt%).

Ternary diagrams based on normative mineralogy (Thompson, 1984) reveal that most of the Eğrikuyu monogenetic field basalts are silica undersaturated (0.3%–5.8% Nph) and plot in the olivine-alkali basalt field, except two more evolved (silica-saturated) Ol-Hyp–normative (1.1%–2.8% Hyp) samples (Fig. 5A). The Quaternary Central Anatolian volcanic province basalts, including the Eğrikuyu monogenetic field basalts (e.g., Ercan et al., 1992; Aydar et al., 1995; Notsu et al., 1995; Deniel et al., 1998; Kürkçüoğlu et al., 1998; Alıcı-Şen et al., 2004; Güçtekin and Köprübaşı, 2009; Kürkçüoğlu, 2010; Aydin et al., 2014; Reid et al., 2017), also plot in both silica-saturated and silica-undersaturated fields (Fig. 5A). In contrast to Pliocene–Quaternary Anatolian basalts from the Eastern Anatolian volcanic province (Pearce et al., 1990; Notsu et al., 1995; Alıcı-Şen et al., 2004; Lustrino et al., 2010, 2012; Özdemir et al., 2011; Ekici et al., 2014; Lebedev et al., 2016; Oyan et al., 2016), which also have both alkaline and subalkaline affinity (Ol-Nph and Ol-Hyp normative), Kula basalts are entirely Ol-Nph normative with strong alkaline affinity (Fig. 5A; Ercan, 1993; Notsu et al., 1995; Aldanmaz, 2002; Alıcı et al., 2002; Innocenti et al., 2005; Tokçaer et al., 2005; Chakrabarti et al., 2012; Grützner et al., 2013). In addition, all Pliocene–Quaternary Anatolian basalts, including the Eğrikuyu monogenetic field, exhibit Na-alkaline affinity (ΔQ = [quartz – {leucite + nepheline + olivine}] < 0) according to the diagram of Foley et al. (1987) (Aydin et al., 2014; Uslular, 2016).

The total alkali versus silica (TAS) diagram of Le Maitre et al. (2002) also revealed the same interpretation obtained using CIPW normative mineralogy for both Eğrikuyu monogenetic field and Anatolian basalts (Fig. 5B). Color-coding is given to all basalts according to their normative composition, either Ol-Hyp normative transitional basalts (TB) or Ol-Nph normative olivine-alkali basalts (AB) (Fig. 5B). AB samples have 47–49 wt% SiO_2 with mildly alkaline to alkaline affinity, whereas TB samples are more evolved (50–51 wt% SiO_2) with subalkaline affinity, based on the division line of Irvine and Baragar (1971) (Fig. 5B). As the exact correlation between TAS and silica saturation has never been achieved due to various planar surfaces in the basalts, a diagram originally proposed by Bellieni et al. (1983) for the separation of subalkali and alkali basalts can be used (Fig. 5B, basalt field with bold line; Le Maitre et al., 2002). AB samples mainly plot on the overlap field in this diagram, suggesting that they are three times as likely to be alkali basalts than subalkali basalts (Fig. 5B). AB with a high normative Nph, on the other hand, plot throughout the alkali field,

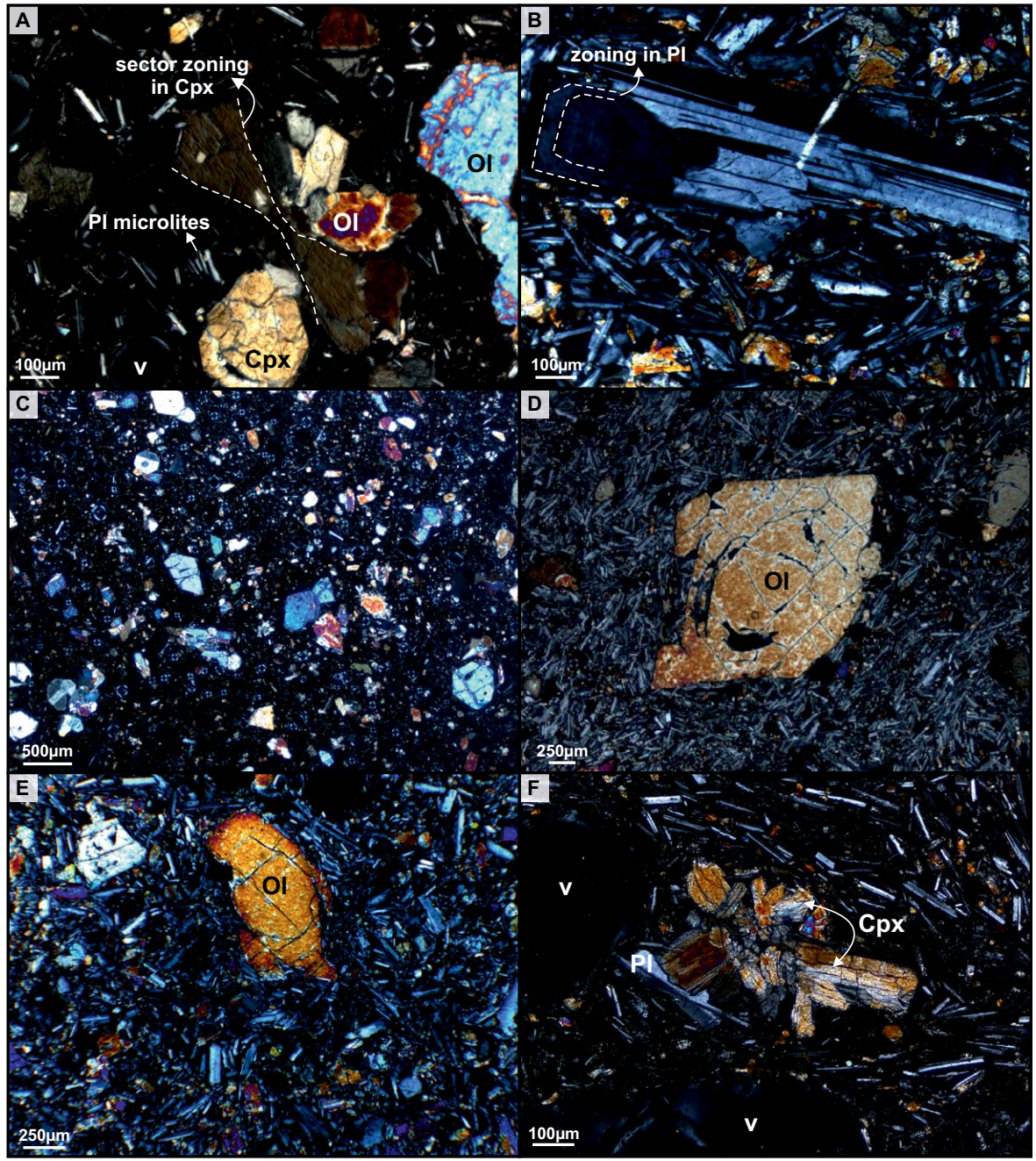

Figure 4. Photomicrographs of Eğrikuyu monogenetic field basalts. (A) Sector (or hourglass) zoning in clinopyroxene (Cpx) with olivine (Ol) microphenocrysts and plagioclase (Pl) microlites. (B) Zoned Pl microphenocryst in a basaltic flow. (C) Olivine-rich basaltic lava flow. (D) Skeletal Ol with pilotaxitic Pl in a lava flow. (E) Skeletal Ol showing compositional difference in its core and rim. (F) Scoria displaying cumulates of Cpx and Ol microphenocrysts. v—vesicle.

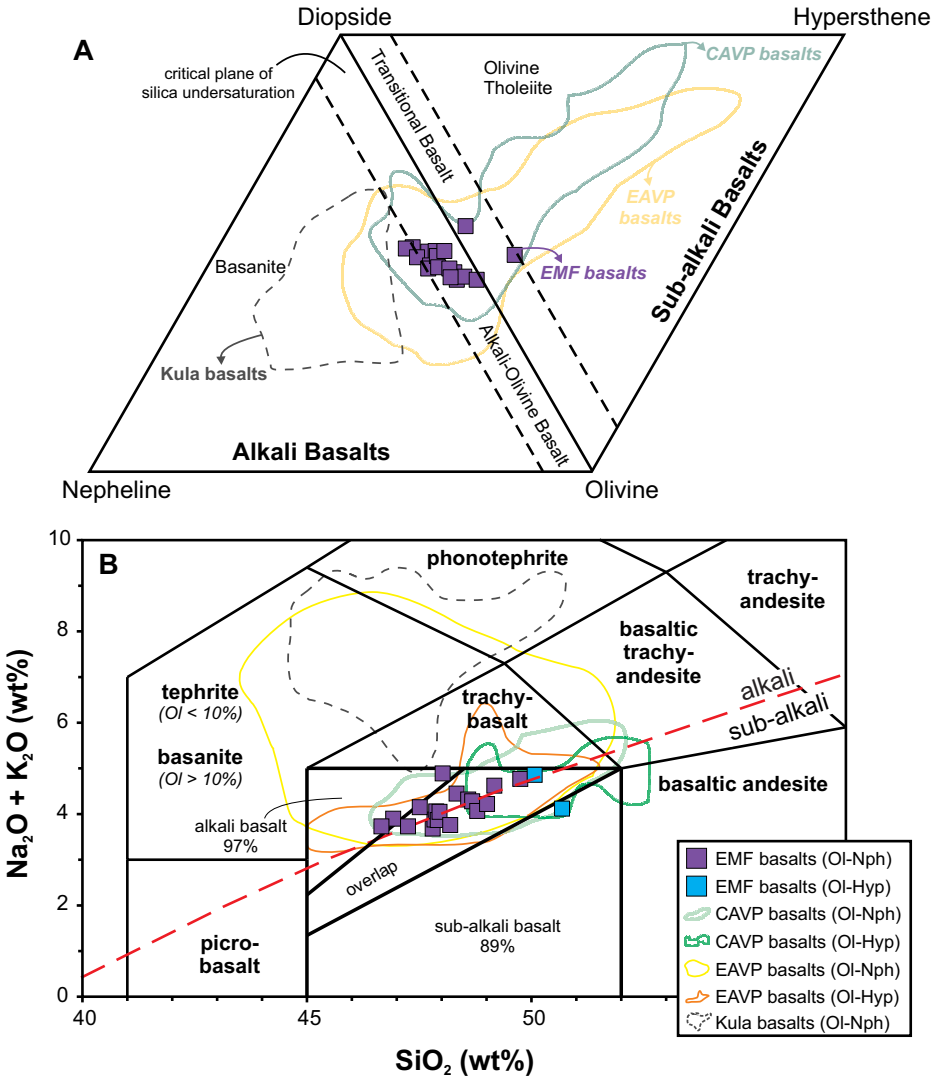

Figure 5. (A) Classification of the Eğrikuyu monogenetic field (EMF) basalts compared to other Pliocene–Quaternary Anatolian basalts (see text for the references) based on CIPW normative composition (Thompson, 1984; Rollinson, 1993). Hyp—hypersthene; Nph—nepheline; Ol—olivine; CAVP—Central Anatolian volcanic province; EAVP—Eastern Anatolian volcanic province. (B) Total alkalis vs. SiO_2 (wt%) diagram (Le Maitre et al., 2002) for the Eğrikuyu monogenetic field basalts in comparison to other Anatolian basalts (see text for the references). Red dashed line separates subalkali and alkali compositions (Irvine and Baragar, 1971). The solid line represents basalt classification of Le Maitre et al. (2002, and references therein). Ol-Nph—olivine-nepheline; Ol-Hyp—olivine-hypersthene.

supporting their strong alkaline affinity. Only one TB sample plots in the subalkali field, implying its subalkali affinity with 89% (Fig. 5B). Except for the Kula basalts, which are exclusively alkaline (i.e., basanite, tephrite, and phonotephrite), most of the Central Anatolian volcanic province (including Eğrikuyu monogenetic field) and Eastern Anatolian volcanic province basalts have transitional to mildly alkaline compositions and plot in the overlap field (Fig. 5B).

The following geochemical interpretation of major-and trace-element and isotope geochemistry data will be envisaged based on the normative classification of both Eğrikuyu monogenetic field and other Anatolian basalts.

Mineral Chemistry and Geothermobarometry

As discussed above, many microphenocrysts found in the Eğrikuyu monogenetic field basalts show disequilibrium textures (e.g., skeletal crystals, reaction rims) mainly related to rapid decompression rather than magma mixing. Therefore, we have avoided selecting minerals that display disequilibrium textures to limit the physical conditions under which magmas were crystallized. Representative Ol, Cpx, Pl, and some Fe-Ti oxide analyses are listed in Table 2.

Estimated pressure and temperature values for Eğrikuyu monogenetic field basalts were calculated using mineral-liquid equilibria based on the calibrations of Putirka et al. (2007) and Putirka (2008). The whole-rock composition was considered as liquid (or melt) composition in the geothermobarometric calculations. In addition, pressure and temperature values were also estimated by using whole-rock composition (Table 3; Lee et al., 2009), and pressure values were used as input for geothermobarometric calculations on mineral chemistry. In order to provide constraints for this simplification and eliminate misleading results (e.g., owing to the high proportion of xenocrysts or cumulates, even when not evident in petrographical observations), we also considered the mineral-liquid equilibrium according to partition coefficient (K_D) tests of Roeder and Emslie (1970). Representative chemical compositions and structural formulae of the minerals were calculated using Microsoft Office Excel macros published at https://serc.carleton.edu/research_education/equilibria/index.html.

The following interpretations and discussions based on the mineral chemistry of the Eğrikuyu monogenetic field basalts are based on their two distinct geochemical affinities (i.e., alkali and transitional basalts).

Olivine

Olivine core composition in the alkali Eğrikuyu monogenetic field basalts ranges between Fo_{64} and Fo_{89} ($Fo = 100 \times Mg/[Mg + Fe_T]$, where T is total iron), whereas the range is Fo_{70}–Fo_{90} in transitional Eğrikuyu monogenetic field basalts (Table 2; Supplemental Data [footnote 1]). Fo contents of Eğrikuyu monogenetic field basalts are also similar with those of the Central Anatolian volcanic province basalts (Aydar et al., 1995; Aydin, 2008; Köprübaşı et al., 2014). The olivine phenocrysts are essentially unzoned, or normally zoned with decreasing Fo content toward the rim (Fig. 6A). Most of the olivine crystals have Mg-rich cores, but they display a relatively sharp decrease in Fo content toward

TABLE 2. REPRESENTATIVE MINERAL (Ol, Cpx, AND Pl) CORE COMPOSITIONS OF EĞRIKUYU MONOGENETIC FIELD BASALTS BY ELECTRON MICROPROBE ANALYSIS

Sample:	GU-1			GU-10			GU-16		
Mineral:	Ol	Cpx	Pl	Ol	Cpx	Pl	Ol	Cpx	Pl
SiO_2	39.58	49.63	51.78	36.62	49.27	50.59	40.46	49.62	48.98
TiO_2	0.03	1.29	0.82	0.05	1.67	0.10	0.00	0.78	0.07
Al_2O_3	0.02	5.07	18.46	0.07	4.23	30.94	0.05	5.45	30.99
FeO^T	13.54	6.80	4.55	22.17	8.29	0.66	9.54	4.59	1.35
MnO	0.23	0.15	0.06	0.37	0.21	0.00	0.13	0.10	0.03
MgO	43.38	14.21	5.03	36.49	13.96	0.14	49.28	15.08	0.04
CaO	0.26	21.62	15.15	0.40	20.63	13.71	0.21	22.62	14.29
Na_2O	0.00	0.38	3.64	0.03	0.43	3.54	0.02	0.45	3.41
K_2O	0.00	0.01	0.35	0.02	0.04	0.21	0.01	0.00	0.47
Cr_2O_3	0.01	0.34	0.02	0.00	0.27	0.00	0.07	1.24	0.02
Total	97.04	99.51	99.85	96.23	99.00	99.89	99.76	99.92	99.65
Si	1.023	1.842	2.370	0.995	1.849	2.305	0.992	1.819	2.241
Ti	0.001	0.036	0.028	0.001	0.047	0.003	0.000	0.022	0.002
Al^T	0.001	0.222	0.995	0.002	0.187	1.662	0.001	0.236	1.671
Al^{IV}	–	0.010	–	–	0.008	–	–	0.036	–
Al^{VI}	–	0.039	–	–	0.043	–	–	0.079	–
Cr	–	0.172	0.001	0.000	0.217	0.000	0.001	0.062	0.001
Fe^{3+}	–	0.005	0.174	0.006	0.007	0.025	0.013	0.003	0.052
Fe^{2+}	0.293	0.786	0.000	0.498	0.781	0.000	0.183	0.824	0.000
Mn	0.005	0.860	0.002	0.009	0.830	0.000	0.003	0.888	0.001
Mg	1.671	0.028	0.343	1.478	0.031	0.010	1.801	0.032	0.003
Ca	0.007	1.842	0.743	0.012	–	0.669	0.006	1.819	0.701
Na	–	–	0.323	–	–	0.313	–	–	0.302
K	–	–	0.021	–	–	0.012	–	–	0.028
Total oxygen	4	6	8	4	6	8	4	6	8
Forsterite	84.57	–	–	73.83	–	–	89.83	–	
Fayalite	14.81	–	–	25.16	–	–	9.76	–	
Wollastonite	–	46.29	–	–	44.34	–	–	47.94	
Enstatite	–	42.34	–	–	41.75	–	–	44.46	
Ferrosilite	–	11.37	–	–	13.91	–	–	7.60	
Anorthite	–	–	68.37	–	–	67.28	–	–	68.01
Albite	–	–	29.73	–	–	31.48	–	–	29.32
Orthoclase	–	–	1.91	–	–	1.24	–	–	2.67

Note: Ol—olivine, Cpx—clinopyroxene, Pl—plagioclase.

the rim (Fig. 6A), with a wide range of composition (Fo_{67} to Fo_{88}), especially in the transitional basalts (Supplemental Data [footnote 1]). The lower Mg rim compositions might be related to rapid cooling or fast growth of the crystals, also evident in petrographic observations (e.g., skeletal olivine; Fig. 4D), or they might be related to the proportion of heterogeneity in the source (i.e., transitional vs. alkali affinity; see whole-rock geochemistry section for further discussion).

Most of the olivine crystals in the Eğrikuyu monogenetic field basalts are not in equilibrium with the melt (Fig. 7A; i.e., outside of $K_D = 0.30 \pm 0.03$), which has also been reported for some Central Anatolian volcanic province basalts (e.g., Köprübaşı et al., 2014), suggesting that olivine crystals either formed as accumulated xenocrysts or crystallized in evolved magmas. However, some of the olivine crystals in Eğrikuyu monogenetic field basalts only plot below the equilibrium boundary (Fig. 7), and therefore they seem to have formed either in a more evolved magma or due to rapid cooling. Mg# versus major oxides (e.g., variable CaO content) plots of olivine crystals (Supplemental Data [footnote 1]) also imply a variety of magmas from different mantle sources, as in the case of Kula basalts (Grützner et al., 2013) and some other basaltic monogenetic fields (e.g., Tenerife—Albert et al., 2015; Kissomlyò monogenetic volcano—Jankovics et al., 2015). Thermometry calculations based on olivine crystals in the Eğrikuyu monogenetic field basalts that equilibrated with the melt yielded temperatures of 1272–1280 °C for TB and 1273–1356 °C for AB.

TABLE 3. WHOLE-ROCK MAJOR- AND TRACE-ELEMENT GEOCHEMISTRY DATA FOR EĞRIKUYU MONOGENETIC FIELD BASALT

Sample:	GU-1	GU-2	GU-3	GU-4	GU-5	GU-6	GU-7	GU-8	GU-9	GU-10
Coordinate (UTM WGS84)	601537E 4185982N	589793E 4190879N	599880E 4187641N	596210E 4191091N	596671E 4191233N	595433E 4191679N	587864E 4184762N	590496E 4200474N	583448E 4189540N	597511E 4201267N
P (GPa)	1.92	1.98	1.93	1.92	2.11	2.13	1.26	2.08	2.03	1.95
T (°C)	1403	1409	1408	1398	1424	1423	1334	1421	1405	1416
Major oxides (wt%)										
SiO_2	49.01	48.19	47.80	48.59	47.84	47.25	50.68	48.68	47.51	50.07
TiO_2	1.07	1.05	0.85	1.15	1.30	1.22	0.79	1.36	1.14	1.40
Al_2O_3	15.83	16.14	14.79	15.93	15.45	15.79	15.15	15.83	15.59	16.39
Fe_2O_3(t)	8.91	8.91	8.91	8.69	9.07	8.95	7.66	9.21	8.65	9.01
MnO	0.14	0.15	0.15	0.14	0.14	0.14	0.12	0.14	0.14	0.14
MgO	9.72	9.77	11.49	9.65	9.75	9.65	9.96	9.42	9.98	7.90
CaO	10.03	10.96	10.51	9.82	10.71	11.06	10.07	9.49	10.81	8.47
Na_2O	3.45	3.12	2.98	3.32	3.09	3.01	3.44	3.33	3.17	3.61
K_2O	0.77	0.64	0.70	1.00	0.79	0.72	0.68	0.95	0.98	1.25
P_2O_5	0.34	0.25	0.28	0.39	0.30	0.29	0.20	0.30	0.29	0.39
LOI	0.30	0.40	1.10	0.90	1.10	1.50	0.80	0.90	1.30	1.00
Sum	99.66	99.66	99.61	99.62	99.64	99.66	99.67	99.67	99.64	99.66
H_2O (Ce/200)	1.01	0.77	1.01	1.28	1.21	0.82	0.67	0.78	0.87	1.02
Mg#	68.36	68.49	71.85	68.73	68.06	68.13	72.04	66.97	69.57	63.46
CIPW Norm										
Quartz	0	0	0	0	0	0	0	0	0	0
Orthoclase	4.61	3.84	4.25	6.03	4.79	4.37	4.08	5.73	5.91	7.56
Plagioclase	51.86	50.78	46.56	51.23	48.85	48.73	54.04	52.69	45.23	56.58
Nepheline	1.95	2.52	2.57	1.96	2.42	3.06	0	1.12	4.53	0
Diopside	18.02	20.16	20.86	16.88	20.77	21.07	20.30	16.16	21.64	12.08
Hypersthene	0	0	0	0	0	0	1.09	0	0	2.84
Olivine	18.72	18.13	21.45	18.83	17.90	17.70	16.79	18.90	17.84	15.28
Magnetite	1.97	1.97	1.99	1.93	2.02	2.00	1.70	2.04	1.93	2.00
Ilmenite	2.07	2.03	1.65	2.22	2.53	2.37	1.54	2.64	2.22	2.72
Apatite	0.81	0.58	0.67	0.93	0.72	0.70	0.46	0.72	0.70	0.93
Sum	100.01	100.01	100	100.01	100	100	100	100	100	99.99
Differentiation index	58.42	57.14	53.38	59.22	56.06	56.16	58.12	59.54	55.67	64.14
Trace element (ppm)										
Rb	13.5	9.7	13.3	17.7	17.0	9.9	10.0	12.6	19.5	23.2
Sr	656	680	689	910	676	655	672	538	736	629
Ba	309	280	335	470	351	265	269	267	386	338
V	193	211	213	188	206	230	176	193	210	179
Cr	369	369	520	342	369	328	486	349	239	253
Co	45.8	44.0	48.5	42.0	45.5	43.7	41.3	40.9	39.1	39.6
Ni	185	148	252	194	191	189	212	173	197	146
Y	22.7	23.5	18.4	20.1	21.4	21.5	15.4	22.5	20.2	23.9
Zr	121	108	81	129	115	117	76	128	98	168
Nb	10.6	8.3	10.5	11.7	11.4	8.6	5.8	9.9	8.1	13.3
La	25.6	18.8	26.2	32.0	32.3	21.0	18.3	19.0	22.0	24.8
Ce	50.5	38.4	50.4	63.9	60.5	41.2	33.5	39.1	43.5	51.2
Pr	5.80	4.62	5.48	7.15	6.45	4.74	3.91	4.70	4.97	6.19
Nd	23.1	18.0	20.7	27.1	24.1	19.0	15.0	18.9	19.9	24.8
Sm	4.5	3.8	3.9	4.7	4.4	3.6	3.0	3.9	4.0	4.8
Eu	1.45	1.24	1.24	1.43	1.34	1.33	1.03	1.37	1.19	1.57
Gd	4.78	4.45	3.79	4.69	4.54	4.37	3.29	4.33	3.98	5.04
Tb	0.68	0.68	0.56	0.67	0.65	0.66	0.49	0.69	0.63	0.77
Dy	4.07	4.01	3.15	3.66	3.93	2.77	4.17	3.59	4.25	4.46
Ho	0.86	0.84	0.65	0.76	0.78	0.80	0.58	0.86	0.73	0.84
Er	2.52	2.35	1.89	2.06	2.09	2.23	1.67	2.65	2.04	2.40
Tm	0.39	0.36	0.30	0.31	0.32	0.35	0.26	0.36	0.31	0.36
Yb	2.48	2.33	1.81	1.99	2.05	2.18	1.63	2.28	2.10	2.27
Lu	0.37	0.37	0.26	0.32	0.31	0.30	0.25	0.35	0.30	0.36
Th	4.9	3.1	4.8	5.5	8.0	3.9	3.2	3.8	3.7	4.3
Pb	2.2	2.9	1.8	2.9	1.2	1.5	1.6	2.5	2.5	2.2
U	1.3	0.8	1.2	1.5	1.7	1.0	0.7	1.0	0.9	1.1
Hf	2.6	2.4	2.1	2.8	2.6	2.4	1.9	2.8	2.4	3.4
Ta	0.5	0.5	0.4	0.6	0.6	0.5	0.2	0.5	0.5	0.7
Ga	14.6	14.7	14.3	13.0	15.1	15.4	14.4	14.2	13.5	16.3
Cs	0.2	0.1	0.4	0.7	0.2	0.4	0.2	0.2	0.5	0.5
La/Sm	5.6	4.9	6.8	6.8	7.4	5.9	6.2	4.9	5.5	5.2
Ba/Nb	29.2	33.7	31.9	40.2	30.8	30.8	46.4	27.0	47.7	25.4
Nb/Yb	0.23	0.28	0.17	0.17	0.18	0.25	0.28	0.23	0.26	0.17
Zr/Hf	46.35	44.88	38.62	46.14	44.19	48.63	40.11	45.61	40.67	49.44

(*continued*)

TABLE 3. WHOLE-ROCK MAJOR- AND TRACE-ELEMENT GEOCHEMISTRY DATA FOR EĞRIKUYU MONOGENETIC FIELD BASALT (*continued*)

Sample:	GU-11	GU-12	GU-13	GU-14	GU-15	GU-16	GU-17	GU-18	GU-19	GU-20
Coordinate (UTM WGS 84)	597683E 4204570N	599400E 4184394N	593305E 4202244N	593572E 4196375N	588560E 4183013N	587845E 4182636N	589092E 4183848N	583254E 4202828N	596062E 4190258N	589477E 4203402N
P (GPa)	2.10	1.86	2.26	2.15	2.11	2.11	2.29	1.79	2.12	2.19
T (°C)	1430	1392	1441	1420	1421	1411	1429	1380	1430	1433
Major oxides (wt%)										
SiO_2	49.75	49.17	47.95	48.02	48.33	46.92	46.66	47.91	48.79	47.88
TiO_2	1.43	1.27	1.32	1.34	1.31	1.15	1.51	1.03	1.12	1.30
Al_2O_3	16.56	16.11	15.50	15.97	15.86	14.62	16.09	15.54	16.70	16.29
Fe_2O_3(t)	9.16	8.60	9.50	8.75	9.00	8.82	9.01	8.39	9.06	9.21
MnO	0.14	0.14	0.15	0.14	0.14	0.14	0.15	0.14	0.14	0.14
MgO	7.95	9.24	9.80	8.21	9.01	11.24	9.64	11.05	8.31	9.23
CaO	8.82	9.46	9.98	9.46	9.87	11.65	11.59	10.76	10.67	9.84
Na_2O	3.71	3.63	3.18	3.50	3.50	2.86	2.75	3.16	3.27	3.26
K_2O	1.06	0.99	0.87	1.39	0.95	1.04	0.98	0.71	0.80	0.80
P_2O_5	0.29	0.37	0.37	0.41	0.40	0.37	0.24	0.23	0.35	0.28
LOI	0.80	0.60	1.00	2.40	1.20	0.70	1.00	0.60	0.40	1.40
Sum	99.68	99.66	99.65	99.63	99.65	99.57	99.65	99.62	99.67	99.66
H_2O (Ce/200)	0.90	0.95	1.00	1.32	1.03	1.23	0.77	0.69	1.03	0.81
Mg#	63.22	68.05	67.14	65.01	66.49	71.62	67.95	72.30	64.50	66.49
CIPW Norm										
Quartz	0	0	0	0	0	0	0	0	0	0
Orthoclase	6.38	5.97	5.26	8.51	5.73	6.26	5.91	4.25	4.79	4.85
Plagioclase	57.27	52.49	50.16	49.07	50.68	38.45	45.07	46.78	54.35	53.20
Nepheline	0.33	2.13	1.83	3.41	2.74	5.80	4.33	3.82	1.48	1.79
Diopside	13.54	16.17	17.80	17.13	17.83	25.67	22.37	21.07	18.16	16.17
Hypersthene	0	0	0	0	0	0	0	0	0	0
Olivine	16.96	18.00	19.40	16.29	17.51	18.76	16.79	19.69	16.24	18.75
Magnetite	2.03	1.90	2.12	1.97	2.00	1.96	2.00	1.86	2.00	2.06
Ilmenite	2.77	2.45	2.56	2.64	2.54	2.22	2.92	1.99	2.17	2.53
Apatite	0.70	0.88	0.88	1.00	0.95	0.88	0.58	0.53	0.83	0.67
Sum	99.98	99.99	100.01	100.02	99.98	100	99.97	99.99	100.02	100.02
Differentiation index	63.98	60.59	57.25	60.99	59.15	50.51	55.31	54.85	60.62	59.84
Trace element (ppm)										
Rb	14.4	14.1	13.1	23.6	14.5	18.5	15.4	10.1	13.5	13.2
Sr	603	668	615	739	656	779	641	647	677	588
Ba	267	309	306	413	388	420	350	410	278	264
V	178	167	208	178	172	229	236	196	206	312
Cr	253	349	342	260	308	479	301	445	274	315
Co	37.6	40.9	44.3	36.1	35.4	45.3	40.5	42	38.2	39.5
Ni	154	189	199	126	171	194	142	223	100	152
Y	23.5	21.2	24.2	23.1	22.4	18.7	21.4	17.8	22.7	21.2
Zr	163	156	142	173	171	102	105	95	123	121
Nb	11.4	13	11.5	11.5	10.6	12.7	9.4	7.2	11.1	9.1
La	21.3	23.1	25.1	31.6	25.2	32.7	19.7	17.3	28.0	20.9
Ce	45.0	47.5	49.9	66.0	51.4	61.6	38.4	34.3	51.4	40.6
Pr	5.51	5.63	5.81	7.82	6.09	7.35	4.66	4.20	5.76	4.78
Nd	21.6	22.9	22.3	30.9	24.3	29.6	18.7	16.8	22.1	19.1
Sm	4.64	4.47	4.43	5.88	4.84	5.24	3.76	3.46	4.19	3.86
Eu	1.57	1.42	1.51	1.72	1.5	1.5	1.26	1.12	1.4	1.23
Gd	4.59	4.42	4.97	5.14	4.61	4.42	4.07	3.32	4.63	3.93
Tb	0.74	0.7	0.73	0.77	0.74	0.61	0.67	0.56	0.69	0.65
Dy	4.46	4.19	4.22	4.37	4.42	3.81	3.88	3.59	4.27	4
Ho	0.86	0.78	0.87	0.87	0.85	0.7	0.77	0.66	0.83	0.78
Er	2.55	2.24	2.44	2.25	2.49	1.81	2.1	1.93	2.43	2.07
Tm	0.38	0.34	0.37	0.33	0.36	0.27	0.35	0.29	0.36	0.31
Yb	2.17	1.96	2.47	2.17	2.15	1.59	2.02	1.66	2.28	1.89
Lu	0.34	0.31	0.37	0.32	0.36	0.27	0.33	0.26	0.36	0.3
Th	3.4	3.2	4.3	5.6	3.6	6.1	2.7	2.8	5.1	4.1
Pb	0.6	2.4	1.0	1.2	1.8	1.9	1.6	0.9	2.4	1.1
U	0.7	0.8	0.9	1.5	1	1.2	0.7	0.7	1.2	1.2
Hf	3.4	3.3	3	3.8	3.7	2.5	2.4	2.3	2.6	2.7
Ta	0.7	0.7	0.6	0.7	0.7	0.5	0.5	0.4	0.7	0.5
Ga	14.8	14.9	15.8	14.8	13.9	14.6	14.2	13.3	15.5	14.6
Cs	0.3	0.4	0.05	0.4	0.3	0.4	0.1	0.2	0.5	0.3
La/Sm	4.6	5.2	5.7	5.4	5.2	6.2	5.2	5.0	6.7	5.4
Ba/Nb	23.4	23.8	26.6	35.9	36.6	33.1	37.2	56.9	25.0	29.0
Nb/Yb	0.19	0.15	0.21	0.19	0.20	0.13	0.21	0.23	0.21	0.21
Zr/Hf	47.85	47.24	47.30	45.45	46.30	40.76	43.88	41.22	47.46	44.74

Note: Mg# and CIPW norms were calculated assuming $Fe_2O_3/FeO = 0.15$. UTM WGS84—Universal Transverse Mercator, World Geodetic System 1984; *P*—pressure; *T*—temperature; LOI—loss on ignition.

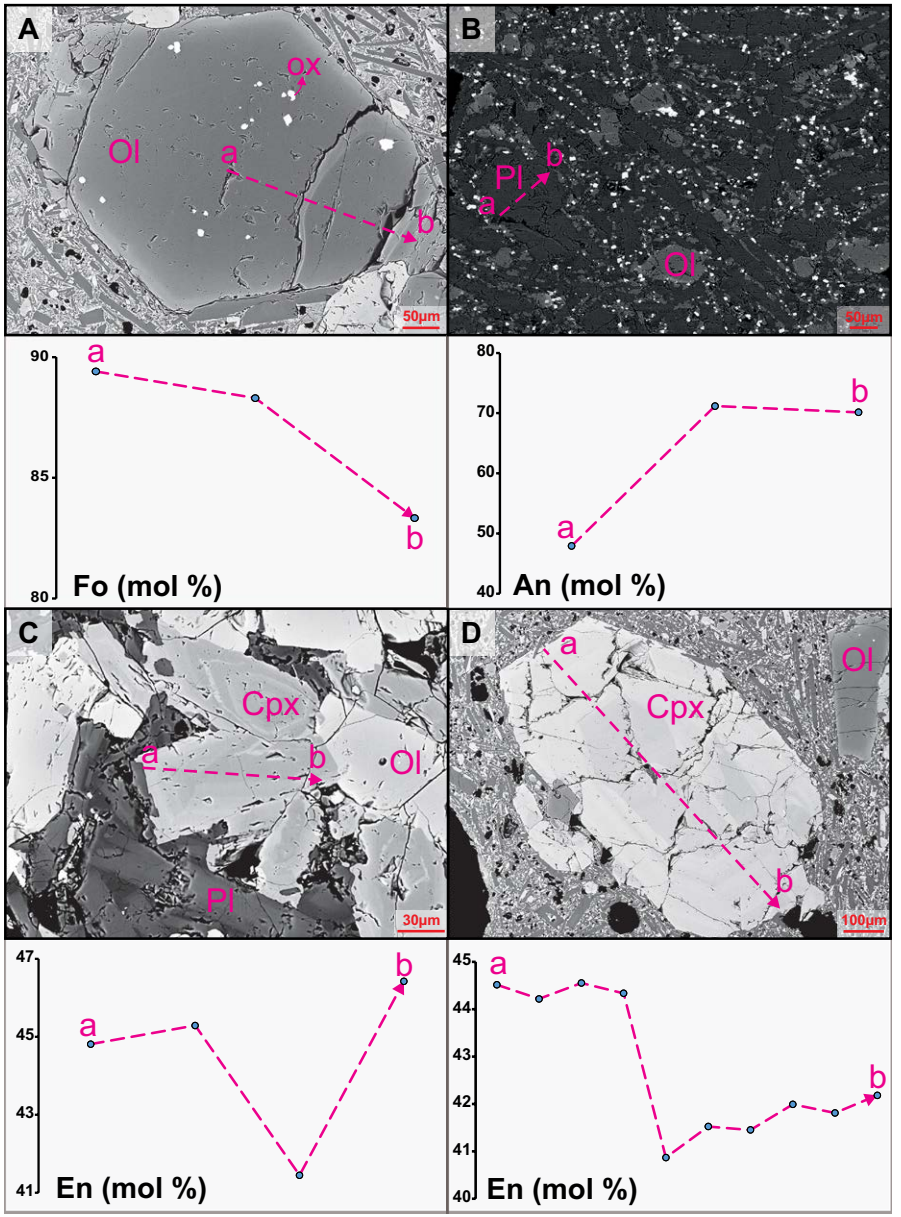

Figure 6. Backscattered electron (BSE) images of Eğrikuyu monogenetic field basalts. (A) Olivine (Ol) microphenocrysts displaying normal zoning with opaque oxide (ox) inclusions. (B) Plagioclase (Pl) microlite showing normal zoning. (C) Sector zoning in clinopyroxene (Cpx) displaying various Mg compositions from rim to rim. (D) Cpx microphenocryst with an Fe-rich core. Fo—forsterite; An—anorthite; En—enstatite.

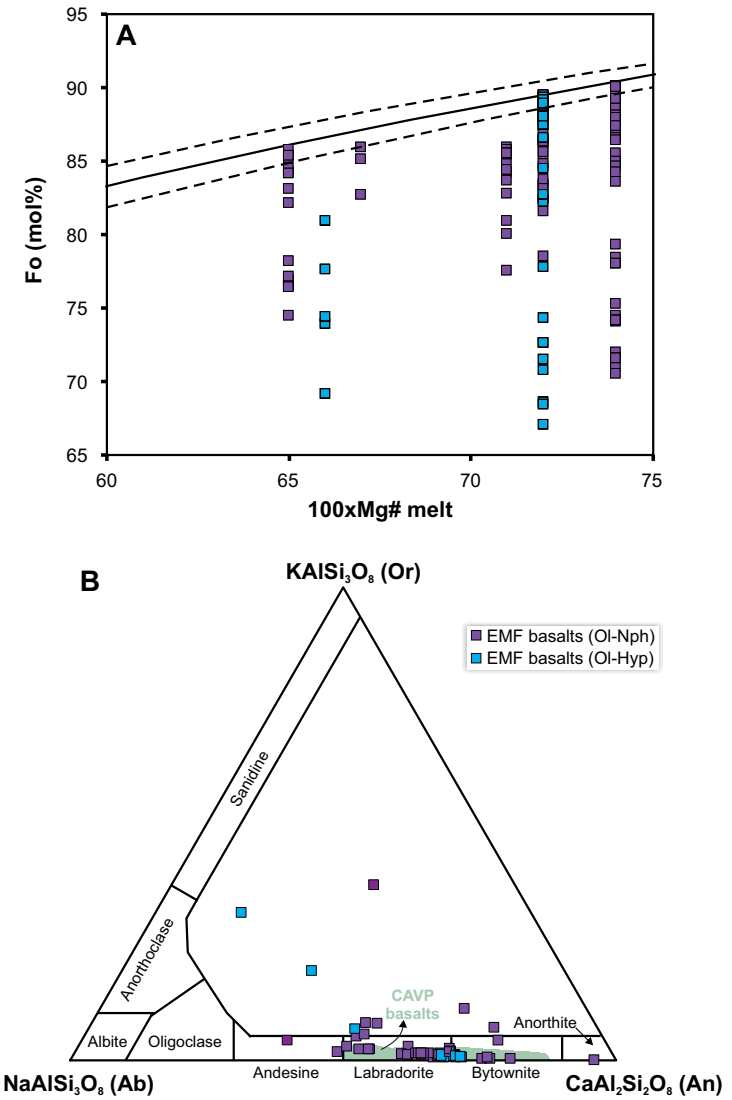

Figure 7. (A) Mineral-melt Fe/Mg equilibrium diagrams for olivine crystals of the Eğrikuyu monogenetic field basalts. Equilibrium field is based on K_D $(Fe\text{-}Mg)^{ol\text{-}liq}$ values (Roeder and Emslie, 1970). (B) Plagioclase (Pl) compositions of Eğrikuyu monogenetic field (EMF) basalts compared to other Central Anatolian volcanic province (CAVP) basalts (Aydar et al., 1995; Aydin, 2008; Köprübaşı et al., 2014; Doğan-Külahçı et al., 2018) plotted on feldspar ternary diagram. Ol-Nph—olivine-nepheline; Ol-Hyp—olivine-hypersthene; Fo—forsterite.

Plagioclase

Anorthite (An) contents range from 37% to 96% in the TB samples and from 16% to 71% in the AB samples (Fig. 6B; Table 2). Most of the plagioclases in the Eğrikuyu monogenetic field basalts is labradorite and bytownite in composition, similar to other Central Anatolian volcanic province basalts (Fig. 7B; Aydar et al., 1995; Aydin, 2008; Köprübaşı et al., 2014; Doğan-Külahçı et al., 2018). Plagioclase crystals of the Eğrikuyu monogenetic field basalts generally display normal zoning (Figs. 4B and 6B), possibly due to the rapid cooling of the magma. The very few plagioclase crystals are in equilibrium with the melt (i.e., out of $K_D = 0.1 \pm 0.11$; Putirka, 2008), as many Pl crystals in the Eğrikuyu monogenetic field basalts are microphenocrysts or microlites. Thermobarometry calculations based on Pl phenocrysts equilibrated with the melt yielded temperatures of 1231–1242 °C and pressures of 5.6–8.4 kbar.

Clinopyroxene

Core-to-rim compositional variation, detected as reverse, oscillatory, and sector (or hourglass) zoning, is a common feature of the pyroxenes in the Eğrikuyu monogenetic field basalts (Figs. 4A, 6C, and 6D). Some of the Cpx crystals in the Eğrikuyu monogenetic field basalts contain high amounts of Al_2O_3 and TiO_2, ranging 3–11 wt% and 0.3–2.8 wt% in AB and 2–7 wt% and 0.5–2 wt% in TB, respectively (Table 2; Supplemental Data [footnote 1]). According to Morimoto (1988), Cpx is mainly diopsidic and rarely augitic in composition ($Wo_{38-45}En_{40-48}Fs_{9-21}$ in TB, and $Wo_{42-50}En_{36-49}Fs_{6-19}$ in AB), similar to other Quaternary Central Anatolian volcanic province basalts (Fig. 8A; Aydar et al., 1995; Aydin, 2008; Köprübaşı et al., 2014; Doğan-Külahçı et al., 2018) and Pliocene Sivas basalts (Kocaarslan and Ersoy, 2018). Cpx is generally ferroan diopside (Fe^{2+} >0.1; Morimoto, 1988) with subordinate ferrian alumina diopside or fassaite (Fe^{3+} >0.1; Morimoto, 1988). Some of the Cpx from AB samples plot with those from alkali basalts (Leterrier et al., 1982), similar to the Kula alkali basalts ($Wo_{45-51}En_{35-45}Fs_{10-17}$; Fig. 8B; Grützner et al., 2013). In addition, some of the AB samples have similar Cpx compositions (i.e., titanian augite and ferrian diopsides) to the Eifel alkali basalts (Duda and Schmincke, 1985). On the other hand, most of the Cpx compositions (ferroan diopside) in the Eğrikuyu monogenetic field and Central Anatolian volcanic province basalts are identical to basaltic rocks in Kissomlyò monogenetic volcano (western Pannonian Basin; Jankovics et al., 2015), where the petrological evolution of postextensional basaltic volcanism (e.g., Harangi et al., 2015) is almost identical to the Central Anatolian volcanic province. The Mg# ($100 \times Mg/[Mg + Fe_T]$, where T is total iron) of the Eğrikuyu monogenetic field basalts ranges from 66 to 89 in the AB samples and 65–84 in the TB samples (Table 2; Supplemental Data [footnote 1]). If only the Fe^{2+} is used for calculation of Mg# ($100 \times Mg/[Mg + Fe^{2+}]$, where Fe^{2+} is calculated from the structural formula), values increase to 70–93. Mg# values are negatively correlated with CaO, Al_2O_3, TiO_2, and Na_2O, whereas Cr_2O_3 contents display almost positive correlation (Supplemental Data [footnote 1]). Abrupt changes in enstatite (En) composition of some Cpx (especially in TB) through the core-to-rim traverses may imply the arrival of more primitive melt (e.g., Albert et al., 2015). The occurrence of Mg-poor Cpx cores (Fig. 6D), especially in the TB samples, also indicates that they may be derived from a different melt source (i.e., in lithospheric mantle) that was subsequently integrated into more primitive magma (e.g., derived from asthenospheric mantle, causing the alkaline affinity in the Eğrikuyu monogenetic field basalts), as in the case of the Kula (Grützner et al., 2013) and Kissomlyó alkali basalts (Jankovics et al., 2015). Although the calculated Fe^{3+} values are high in some Cpx, possibly due to growth kinetics (Mollo et al., 2010), most of the Cpx in the Eğrikuyu mono-

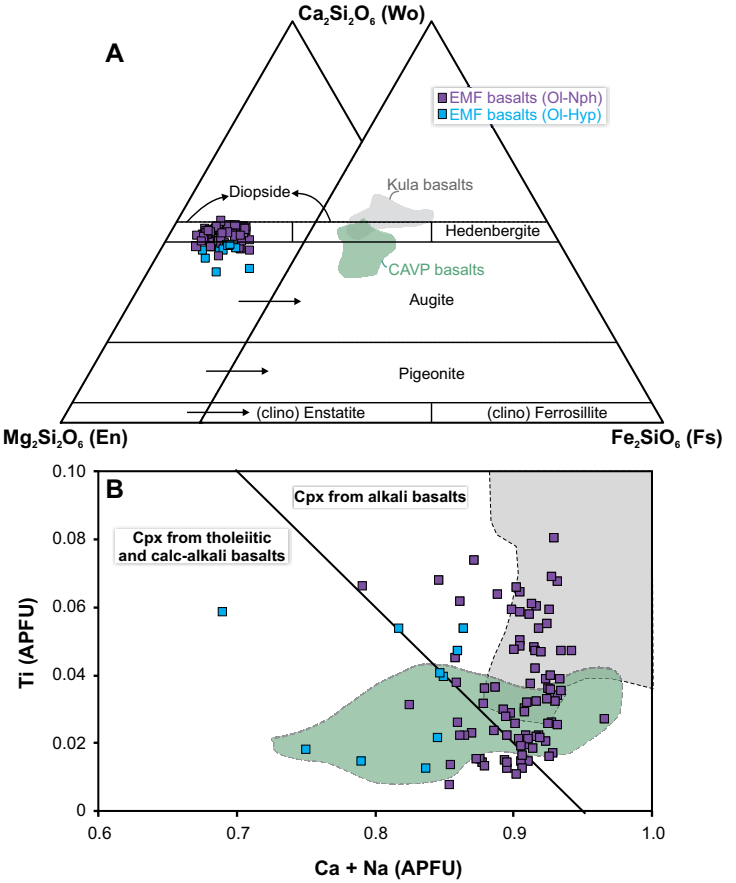

Figure 8. (A) Chemical composition of clinopyroxene (Cpx) in Eğrikuyu monogenetic field (EMF) basalts in comparison to Central Anatolian volcanic province basalts in the pyroxene classification diagram (Morimoto, 1988). (B) Alkali vs. subalkali discrimination diagram based on clinopyroxene compositions (Leterrier et al., 1982) showing clinopyroxene of Eğrikuyu monogenetic field, Central Anatolian volcanic province (CAVP; Aydar et al., 1995; Güçtekin and Köprübaşı, 2009), and Kula basalts (Grützner et al., 2013). Ol-Nph—olivine-nepheline; Ol-Hyp—olivine-hypersthene.

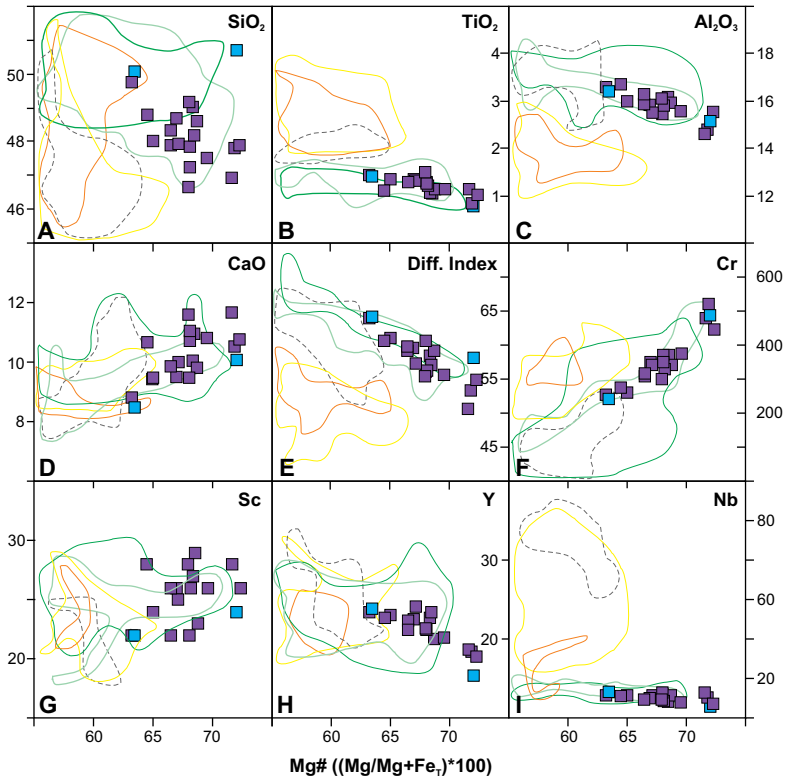

Figure 9. Mg# vs. major-element (wt%) and trace-element (ppm) compositions of Eğrikuyu monogenetic field and other Anatolian basalts (see text for the references). Symbols and lines are as in Fig. 5B.

genetic field basalts has lower Fe^{3+} compared to Fe^{2+}, reflecting the effect of oxidation state in its evolution. Therefore, very few Cpx crystals in the Eğrikuyu monogenetic field basalts (only those from the AB samples) are in equilibrium with the melt (i.e., outside of K_D = 0.27 ± 0.03), and these were used for the geothermometry and geobarometry calculations. Thermobarometry calculations on the Cpx of Eğrikuyu monogenetic field basalts (those in equilibrium with the melt), using calibrations of Putirka (2008), yielded temperatures of 1235–1272 °C and pressures of 4.7–8.3 kbar.

Fe-Ti Oxides

Most of the Fe-Ti oxide microlites and inclusions in major phenocryst phases (e.g., olivine; Fig. 6A) are close to the binary solid solution series of hematite and ilmenite, whereas some plot along the magnetite-ulvospinel line (Supplemental Data [footnote 1]).

Whole-Rock Geochemistry

The geochemistry data of the Anatolian basalts (45–52 wt% SiO_2) of Pliocene–Quaternary age, including the Kula, Central and Eastern Anatolian volcanic province basalts, were compiled to discuss possible similarities with the Eğrikuyu monogenetic field basalts in terms of petrological evolution. In addition, geochemical features of Miocene–Pliocene Anatolian (Central and Eastern Anatolian volcanic province) basalts, circum-Mediterranean anorogenic Cenozoic igneous (CiMACI) basalts, and Aegean arc basalts (Santorini and Nisyros) were also added for comparison in order to better interpret the temporal and petrological evolution of the Eğrikuyu monogenetic field basalts.

Major- and Trace-Element Geochemistry

Eğrikuyu monogenetic field basalts are quite primitive, with comparably high Mg numbers (63–72; Mg# = 100 × Mg/[Mg + Fe_T], where T is to total iron, and Fe^{3+}/Fe_T = 0.15) and MgO contents (7.9–11.5 wt%; Fig. 9; Table 2). Sample GU-16 is probably the most primitive Central Anatolian volcanic province basalt, with a high Mg# (~72) and high MgO (11.2 wt%), and low SiO_2 (46.9 wt%) and $^{87}Sr/^{86}Sr$ contents (0.7046; Tables 3 and 4). The Central Anatolian volcanic province and Eğrikuyu monogenetic field basalts have higher Mg# values compared to other Anatolian basalts (Fig. 9). TB samples are more evolved (50.1–50.7 wt% SiO_2), with almost identical major-element composition to AB samples (46.7–49.8 wt% SiO_2; Fig. 9A). There is a negative trend in Mg# versus some major oxides (Figs. 9A, 9B, and 9C) in the evolved Eğrikuyu monogenetic field basalts (Mg# < 68), suggesting that fractionated phases (Ol + Cpx ± Pl) played a role in magma differentiation. However, Eğrikuyu monogenetic field basalts with high Mg# display scattered patterns in all major-element diagrams, indicating that fractionation had a negligible or only minor effect on basalt genesis (even for the most evolved sample, GU-19, with 50.7 wt% SiO_2; Figs. 9A–9D). The role of differentiation in the evolution of the Eğrikuyu monogenetic field basalts can also be discussed by using the differentiation index of Thornton and Tuttle (1960) (the ratio of normative Qtz, Ab, Or, Nph, Lct, Kls, Na_2CO_3, and Na_2SO_4 to the weight total of the norm). The differentiation index of more evolved Eğrikuyu monogenetic field basalts decreases with increasing Mg# (Fig. 9E), whereas those of relatively primitive basalts have scattered patterns, as in the case of major-element binary diagrams. Comparison of the major-element composition of the Eğrikuyu monogenetic field basalts with other Anatolian basalts also revealed the low TiO_2 contents of the Eğrikuyu monogenetic field (0.8–1.5 wt%) and other Central Anatolian volcanic province basalts in general (0.8–2.1 wt%; Fig. 9B). This might be related to a distinct source composition of the Central Anatolian volcanic province basalts (e.g., rutile-bearing mantle source). The negligible effect of fractionation and scattered patterns of differentiation index, especially in the genesis of comparably primitive Eğrikuyu monogenetic field basalts, suggest that other processes may have been at play (i.e., variable melting degrees and/or heterogeneity in the mantle source, crustal assimilation, and/or sediment input), beyond the

TABLE 4. Sr-Nd-Pb ISOTOPE GEOCHEMISTRY OF THE EĞRIKUYU MONOGENETIC FIELD BASALTS

Sample	$^{87}Sr/^{86}Sr \pm 2\sigma$	$^{143}Nd/^{144}Nd \pm 2\sigma$	ε_{Nd}	$^{206}Pb/^{204}Pb \pm 2\sigma$	$^{207}Pb/^{204}Pb \pm 2\sigma$	$^{208}Pb/^{204}Pb \pm 2\sigma$	Δ7/4	Δ8/4	Age (Ma)
GU-2	0.704941 ± 0.000015	0.512775 ± 0.00002	2.69	18.7749 ± 0.0036	15.6089 ± 0.0030	38.7682 ± 0.0074	8.27	44.24	
GU-4	0.705368 ± 0.000018	0.512736 ± 0.00002	1.93	18.7865 ± 0.0020	15.6083 ± 0.0017	38.8045 ± 0.0062	8.09	41.79	
GU-9	0.705243 ± 0.000006	0.512751 ± 0.00002	2.22	18.7191 ± 0.0158	15.6762 ± 0.0132	39.0990 ± 0.0330	15.61	84.07	
GU-10	0.704627 ± 0.000010	0.512775 ± 0.00002	2.69	18.7236 ± 0.0034	15.5934 ± 0.0028	38.6843 ± 0.0071	7.28	42.05	0.47*
GU-12	0.704520 ± 0.000020	0.512815 ± 0.00002	3.47	18.7561 ± 0.0014	15.5970 ± 0.0012	38.7014 ± 0.0030	7.28	39.82	
GU-14	0.704411 ± 0.000012	0.512804 ± 0.00001	3.25	18.8267 ± 0.0121	15.6570 ± 0.0100	38.8937 ± 0.0253	12.51	50.52	
GU-16	0.704615 ± 0.000013	0.512736 ± 0.00003	1.93	18.7763 ± 0.0038	15.6036 ± 0.0032	38.7455 ± 0.0079	7.72	41.79	
GU-18	0.704960 ± 0.000018	0.512802 ± 0.00002	3.21	18.8273 ± 0.0061	15.5994 ± 0.0051	38.7581 ± 0.0127	6.75	36.89	
GU-19	0.705036 ± 0.000016	0.512704 ± 0.00002	1.30	18.8260 ± 0.3055	15.6108 ± 0.0025	38.8045 ± 0.0062	7.91	41.68	
GU-20	0.704797 ± 0.000015	0.512780 ± 0.00002	2.78	18.8821 ± 0.0062	15.6729 ± 0.0052	38.9598 ± 0.0130	13.51	50.43	

*Age data from Reid et al. (2017).

possible minor fractionation of Ti-bearing minerals, to explain the low-TiO_2 characteristics of the Central Anatolian volcanic province and Eğrikuyu monogenetic field basalts.

Eğrikuyu monogenetic field basalts have relatively higher Cr (~253–520 ppm; Fig. 9F) and Ni (~100–226 ppm; Table 3) contents compared to other Anatolian basalts, reinforcing their almost primitive composition. The role of Ol fractionation in the differentiation of more evolved samples is also apparent (positive correlation between Cr and Mg#; Fig. 9F). The Sc contents (22–29 ppm) are generally scattered or display a slight positive correlation with increasing Mg#, possibly indicating minor fractionation of Cpx in the evolution of Eğrikuyu monogenetic field basalts (Fig. 9G). The most primitive Eğrikuyu monogenetic field basalt (GU-16) has a high Sc content (28.3 ppm), consistent with its elevated CaO/Al_2O_3 value. The incompatible elements of the Eğrikuyu monogenetic field basalts poorly correlate with Mg#, except for Y (15.4–24.2 ppm), which shows a mildly negative trend as a possible indicator of apatite fractionation (Fig. 9H); this might also be related to the enrichment of Y in the residual liquid (e.g., Pearce and Norry, 1979). The Nb content of Eğrikuyu monogenetic field (5.8–13.3 ppm) and Central Anatolian volcanic province (6.2–20.4 ppm) basalts is also comparatively low (Fig. 9I), consistent with the low TiO_2 content (Fig. 9B). The low P_2O_5 (0.2–0.4 wt%) and Ta (0.2–0.7 ppm) contents with enrichment in large ion lithophile elements (LILEs; Rb, Ba, Th, U) also suggest a subduction-related geochemical affinity for the Eğrikuyu monogenetic field basalts, which is also evident in multi-element diagrams normalized to both primitive mantle (PM) and mid-ocean-ridge basalt (MORB), which show depletion in Nb, Ta, P, and Ti (Figs. 10A and 10C). AB samples also show a slight depletion in Y and Yb anomalies in the multi-element diagrams, possibly indicating the occurrence of garnet in the source (Figs. 10A and 10C). The PM-normalized REE patterns of the Eğrikuyu monogenetic field basalts display light (L) REE enrichment (La/Sm ~6) and relatively flat middle (M) REE to heavy (H) REE patterns (Dy/Yb ~2), which are also evident in other Anatolian basalts (Fig. 10E). The almost linear trend in Eu indicates that plagioclase is not the primary fractionating mineral phase, as documented as well in the variation diagrams (Figs. 9C, 9D, and 10E).

The Kula and Eastern Anatolian volcanic province alkali basalts (Ol-Nph normative) display an OIB-like pattern in the PM-normalized multi-element diagram (Fig. 10C). Decompression of a mainly asthenospheric mantle source, with or without the limited contribution of a lithospheric mantle component, has been suggested as the possible mechanism that explains the OIB-like geochemical affinity of these basalts (e.g., Alıcı et al., 2002; Keskin, 2007; Aldanmaz et al., 2015). In addition, CiMACI basalts (Lustrino and Wilson, 2007) and Miocene–Pliocene–age Central (including Koçdağ and Develidağ samples; Kürkçüoğlu et al., 1998; Kürkçüoğlu, 2010) and Eastern Anatolian volcanic province (Karacadağ basalts; Lustrino et al., 2010, 2012; Ekici et al., 2012, 2014) basalts are also compared to Eğrikuyu monogenetic field basalts in both multi-element and REE diagrams (Figs. 10B, 10D, and 10F). While CiMACI basalts display typical signatures of anorogenic magmatism with OIB-like patterns (hump in Nb and Ta, and depletion in K) in multi-element diagrams, almost all Miocene–Pliocene Anatolian basalts, including those with both transitional (Ol-Hyp normative) and alkaline (Ol-Nph normative) geochemical affinity, have slight or explicit depletion in Nb, Ta, Ti, and P anomalies that are consistent with a subduction signature (Figs. 10B and 10D). The enrichment in LILEs and LREEs is also evident as in the Pliocene–Quaternary Anatolian basalts (Fig. 10F). The possible source and geodynamic implications of both Miocene–Pliocene and Pliocene–Quaternary Anatolian basalts are discussed in detail in the following sections.

Isotope Geochemistry

Sr-Nd-Pb isotope compositions of selected Eğrikuyu monogenetic field basalts (10 samples) are presented in Table 4 and plotted in Figure 11. The published isotope data from Pliocene–Quaternary Anatolian basalts (Pearce et al., 1990; Notsu et al., 1995; Deniel et al., 1998; Kürkçüoğlu et al., 1998; Alıcı et al., 2002; Alıcı-Şen et al., 2004; Lustrino et al., 2010; Chakrabarti et al., 2012; Aydin et al., 2014; Ekici et al., 2014; Reid et al., 2017), Aegean arc basalts (Santorini and Nisyros; Buettner et al., 2005; Bailey et al., 2009; Klaver et al., 2016), and

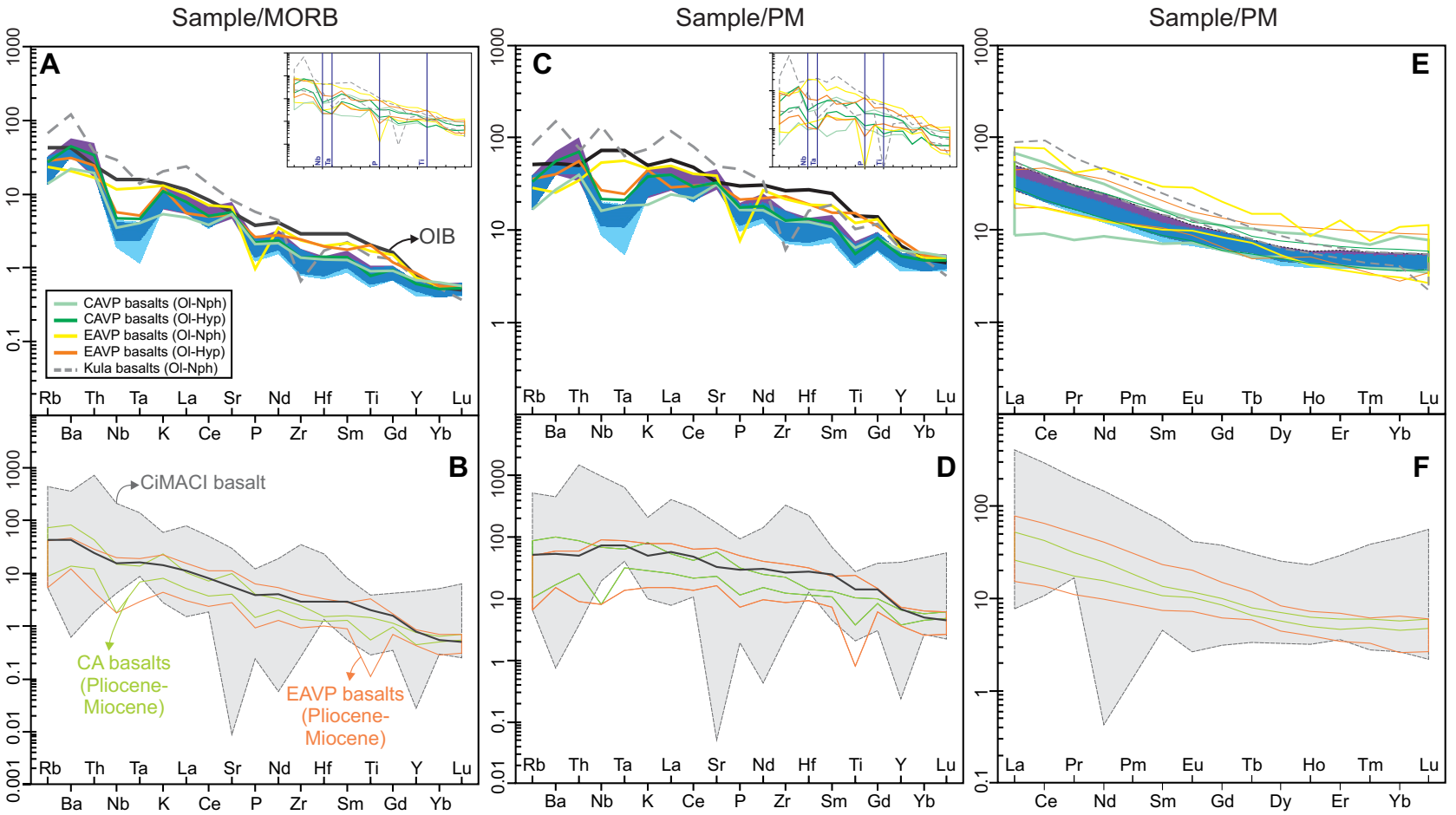

Figure 10. (A) Mid-ocean-ridge basalt (MORB)–normalized multi-element patterns of the Eğrikuyu monogenetic field and other Pliocene–Quaternary Anatolian basalts (average data are considered). (B) Miocene–Pliocene Central Anatolian (CA) and circum-Mediterranean anorogenic Cenozoic igneous (CiMACI) basalts (see text for the references). (C–D) Primitive mantle (PM)–normalized multi-element diagrams. (E–F) PM-normalized rare earth element (REE) diagrams. Normalization values are from Sun and McDonough (1989). Insets in A and C show multi-element patterns of the whole data set of Pliocene–Quaternary Anatolian volcanics. CAVP—Central Anatolian volcanic province; EAVP—Eastern Anatolian volcanic province; Ol-Nph—olivine-nepheline; Ol-Hyp—olivine-hypersthene; OIB—oceanic-island basalt.

Eastern Mediterranean Sea (Klaver et al., 2015) sediments were also included in the diagrams to attain a better source characterization of the Eğrikuyu monogenetic field basalts.

The Eğrikuyu monogenetic field basalts are represented by less radiogenic Sr ($^{87}Sr/^{86}Sr$ = 0.704411–0.705368) and more radiogenic Nd ($^{143}Nd/^{144}Nd$ = 0.512704–0.512815) compositions, similar to other Anatolian and Aegean arc basalts, and they are close to OIB composition (Fig. 11A). However, the Eğrikuyu monogenetic field basalts are clearly distinguished from the CiMACI and Kula basalts, which were derived from a mainly depleted mantle source with a strong OIB-like affinity (Lustrino and Wilson, 2007; Aldanmaz et al., 2015). The heterogeneity in the mantle source of the Eğrikuyu monogenetic field basalts (i.e., depleted and enriched mantle end members) and the contribution of Eastern Mediterranean Sea sediments are also apparent in Figure 11A, which bears similarities to the evolution of Aegean arc basalts (Klaver et al., 2016). The Pb isotope compositions of Eğrikuyu monogenetic field basalts also yield a limited range, with $^{206}Pb/^{204}Pb$ = 18.7191–18.8821, $^{207}Pb/^{204}Pb$ = 15.5934–15.6762,

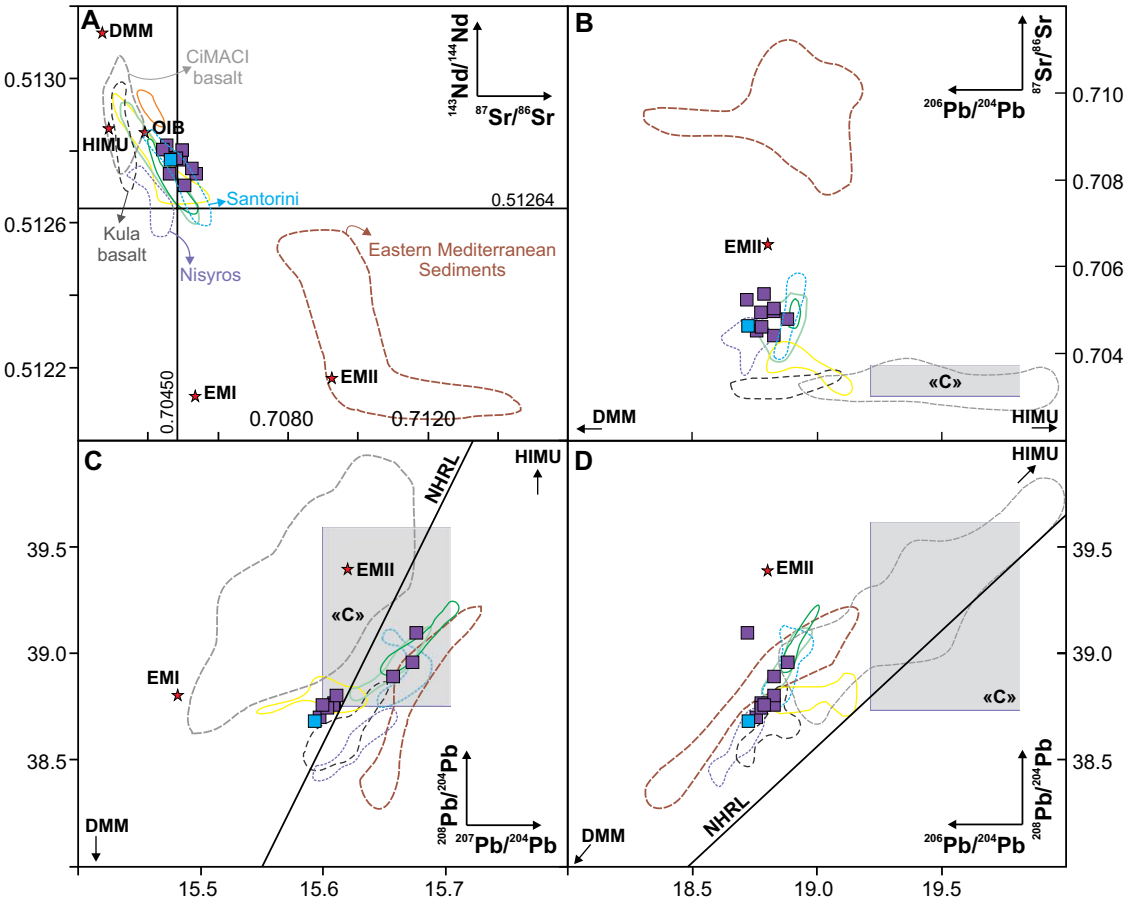

Figure 11. (A) $^{87}Sr/^{86}Sr$ vs. $^{143}Nd/^{144}Nd$ isotope diagram of the Eğrikuyu monogenetic field, Anatolian, Aegean, and circum-Mediterranean anorogenic Cenozoic igneous (CiMACI) basalts, and Eastern Mediterranean Sea sediments. (B) $^{206}Pb/^{204}Pb$ vs. $^{87}Sr/^{86}Sr$. (C) $^{207}Pb/^{204}Pb$ vs. $^{208}Pb/^{204}Pb$. (D) $^{206}Pb/^{204}Pb$ vs. $^{208}Pb/^{204}Pb$. "C"—"Common" mantle from Hanan and Graham (1996). Normalization values and oceanic-island basalt (OIB) compositions are from Sun and McDonough (1989). DMM—depleted mid-ocean-ridge basalt (MORB) mantle (Workman and Hart, 2005). HIMU—high μ (where μ = $^{238}U/^{204}Pb$), EMI and EMII—enriched mantle I and II (Zindler and Hart, 1986; Lustrino and Dallai, 2003). NHRL—Northern Hemisphere reference line (Hart, 1984).

and $^{208}Pb/^{204}Pb$ = 38.6843–39.0990 ratios, except three samples that have relatively high Pb-isotope ratios (Table 4) owing to either source heterogeneity or crustal/lithospheric contamination. On the other hand, most of the Eğrikuyu basalts sampled in this study have distinct $^{207}Pb/^{204}Pb$ ratios that resemble the Kula and Eastern Anatolian volcanic province basalts, but they are lower than the previously published ratios of other Eğrikuyu monogenetic field and Central Anatolian volcanic province basalts (Aydin et al., 2014; Reid et al., 2017). The Eğrikuyu basalts, in general, have a comparable Pb-isotope composition with the Kula basalts, but they have a higher Sr-isotope composition (Fig. 11B). They are isotopically enriched (Δ7/4 ~9.5 and Δ8/4 ~47.3) compared to depleted mantle with respect to the Northern Hemisphere reference line (NHRL; Figs. 11C and 11D; Hart, 1984). Except for some of the Eastern Anatolian volcanic province, Kula, and Eğrikuyu monogenetic field basalts, all remaining basalts have slightly to very high $^{207}Pb/^{204}Pb$ ratios (Fig. 11C), also supporting the role of subducted sediments (Eastern Mediterranean Sea; Klaver et al., 2016; Reid et al., 2017) in their evolution.

The Pb-isotope compositions of the Eğrikuyu monogenetic field basalts do not strictly resemble the common component ("C") mantle composition Hanan and Graham, 1996), but most of the Anatolian basalts are close to the "C" mantle, given their higher $^{207}Pb/^{204}Pb$ contents (Fig. 11C). Although the contribution of sediments in melting is requirement for most Anatolian basalts that resulted in elevated $^{207}Pb/^{204}Pb$ ratios, the idea of possible "C" mantle-like composition of the regional asthenosphere may not be neglected (Gall et al., 2014, and references therein). On the other hand, most CiMACI basalts (Lustrino and Wilson, 2007) are prominently similar to "C" mantle-like isotopic compositions (Figs. 11C and 11D), probably due to their deep asthenospheric sources.

Source Characteristics

The possible source(s) for the generation of Quaternary Central Anatolian volcanic province basalts (including the Eğrikuyu monogenetic field) have been discussed in the literature for decades (Ercan et al., 1992; Notsu et al., 1995; Kürkçüoğlu et al., 1998; Alıcı-Şen et al., 2004; Aydin, 2008; Gençalioğlu-Kuşcu and Geneli, 2010; Gençalioğlu-Kuşcu, 2011; Aydin et al., 2014; Reid et al., 2017). The strong subduction signature (depletion in Nb, Ta, P, and Ti; Fig. 10) and the transitional (Ol-Hyp normative) and mildly alkaline affinity (Ol-Nph normative) of the Central Anatolian volcanic province basalts elicit contentious ideas regarding their mantle source and possible geodynamic origin (e.g., Gençalioğlu-Kuşcu, 2011; Aydin et al., 2014). The common idea on the evolution of these basalts is that they were mainly derived from subcontinental lithospheric mantle metasomatized by the fluids of earlier subduction, with a contribution from upwelling asthenospheric mantle (e.g., Deniel et al., 1998; Alıcı-Şen et al., 2004; Gençalioğlu-Kuşcu and Geneli, 2010). Recently, Reid et al. (2017) proposed three distinct source components for the Central Anatolian volcanic province (especially for the Eğrikuyu monogenetic field) basalts, namely, subduction-modified mantle (SMM), Central Anatolia ambient upper mantle (AUM), and an intraplate-like component (IPC). SMM was also previously defined as "inherited subduction-enrichment" from a previous subduction event in the history of Central Anatolia for the genesis of Central Anatolian volcanics. The AUM component was identified as enriched MORB-like mantle beneath Central Anatolia (Reid et al., 2017). On the other hand, IPC is represented by the Kula basalts (Reid et al., 2017), which have melts of intraplate-like asthenosphere unmodified by subduction enrichment, and possibly raised through a slab tear (Gans et al., 2009; Biryol et al., 2011; Aldanmaz et al., 2015). In this section, we will discuss the relative importance and role of these three components in the generation of monogenetic basaltic volcanism within the Eğrikuyu monogenetic field by using mineral, trace-element, and isotope geochemistry in comparison to other Pliocene–Quaternary basalts in and around Anatolia.

Geochemical Indications of Mantle Enrichment

The Sr anomaly ($Sr^* = Sr_N/\sqrt{[Pr_N \times Nd_N]}$, where N stands for normalization to PM of Sun and McDonough, 1989; McGee et al., 2013) of some Eğrikuyu monogenetic field basalts displays positive trends with K/La, possibly indicating interaction with metasomatized sources or fluids (Fig. 12A). This is in accord with the role of Eastern Mediterranean Sea sediments (Klaver et al., 2015), an important metasomatization agent in the evolution of the Central Anatolian volcanic province and Eğrikuyu monogenetic field basalts (Reid et al., 2017). In addition, the contribution of amphibole in the source of Central Anatolian volcanic province basalts (Reid et al., 2017) can be traced by the higher K/La ratios of some Eğrikuyu monogenetic field basalts (Fig. 12A) and also lower La/Sm ratios (Table 3). However, Eğrikuyu monogenetic field basalts have higher Al_2O_3/TiO_2 (~11–19) ratios compared to alkali basalts (OIB-like) derived from melting of amphibole-bearing metasomatic veins (e.g., Pilet, 2015). Some of the Eğrikuyu monogenetic field basalts (especially Ol-Nph normative ones) have higher Th/Yb ratios, implying a residual garnet-rich source for magma genesis due to either heterogeneity in the mantle source or subduction enrichment (Fig. 12B). MREE/HREE ratios of the Eğrikuyu monogenetic field basalts (e.g., higher Sm/Yb ~2.1, Tb/Yb ~0.3, and Dy/Yb_N ~1.2 with respect to normal [N] MORB) also suggest that garnet remains in the residual phase. The ratios of Nb/Y or Nb/Yb (not shown) can be used as a proxy for mantle enrichment, and the Central Anatolian volcanic province basalts, including some of the Eğrikuyu monogenetic field basalts, seem to be derived from an enriched source, as illustrated in the diagram with respect to Ti anomaly ($Ti^* = Ti_N/\sqrt{[Hf_N \times Sm_N]}$, where N stands for normalization to PM; Fig. 12C; McGee and Smith, 2016). The Central and Eastern Anatolian volcanic province basalts are clearly distinguished from Kula basalts, which have a strong within-plate signature (Fig. 12C). The Zr/Hf and Nb/Ta ratios are important proxies for understanding crust-mantle differentiation (i.e., enriched mantle source via subduction and crustal recycling; Figs. 12D and 12E; Pfänder et al., 2007, 2012; McGee and Smith, 2016). The Eğrikuyu monogenetic field basalts have Zr/Hf ratios between 38.6 and 49.4, and variable Ti*, possibly suggesting a heterogeneity and/or lower-degree melting in the source (Fig. 12D; e.g., Pfänder et al., 2007). The Eğrikuyu monogenetic field basalts also have rather depleted Nb (5.8–13.3 ppm) and Ta (0.2–0.7 ppm) contents compared to continental basalts and OIBs of Pfänder et al. (2007). In addition, Nb/Ta ratios decrease with Zr/Nb ratios in a negative trend (Fig. 12E), indicating different degrees of partial melting. Some samples with high Ba and Th contents (i.e., GU-3, GU-7, and GU-16; Table 3) are also characterized by elevated Nb/Ta ratios (Fig. 12E), and these might reflect the role of crust-mantle differentiation (e.g., Pfänder et al., 2007). High Zr/Y ratios (Pearce, 1983) of the Eğrikuyu monogenetic field and Central Anatolian volcanic province basalts also favor enrichment by subduction. The common location of most of the Eğrikuyu monogenetic field (except the three mentioned above) and Central Anatolian volcanic province basalt data in the PM field in Figures 12E and 12F might be indicative of earlier PM-like compositions before any subduction-related enrichment, similar to late Miocene mafic lavas of western Anatolia (Ersoy et al., 2012).

On the other hand, lower Zr/Nb and elevated Nb/Ta and Th/Yb ratios for the most primitive samples (GU-3 and GU-16; Figs. 12B and 12E) plotted in the Eastern Mediterranean Sea sediment field (Fig. 13B) can be explained by either strong subduction enrichment or crustal/lithospheric contamination. Fractionation of Cpx can also increase the Nb contents and Nb/Ta and Zr/Hf ratios in basalts (Pfänder et al., 2007), but a slight Cpx fractionation of the Eğrikuyu monogenetic field and Central Anatolian volcanic province basalts (Fig. 9) cannot result in such elevated anomalies. In addition, bulk mixing of PM-like composition (Sun and McDonough, 1989) with Eastern Mediterranean Sea sediments (even if it is an unrealistic model due to the involvement of subducted sediments in the melt as either sediment-released fluid or melt) may explain the source enrichment in Eğrikuyu monogenetic field basalts (Fig. 13A).

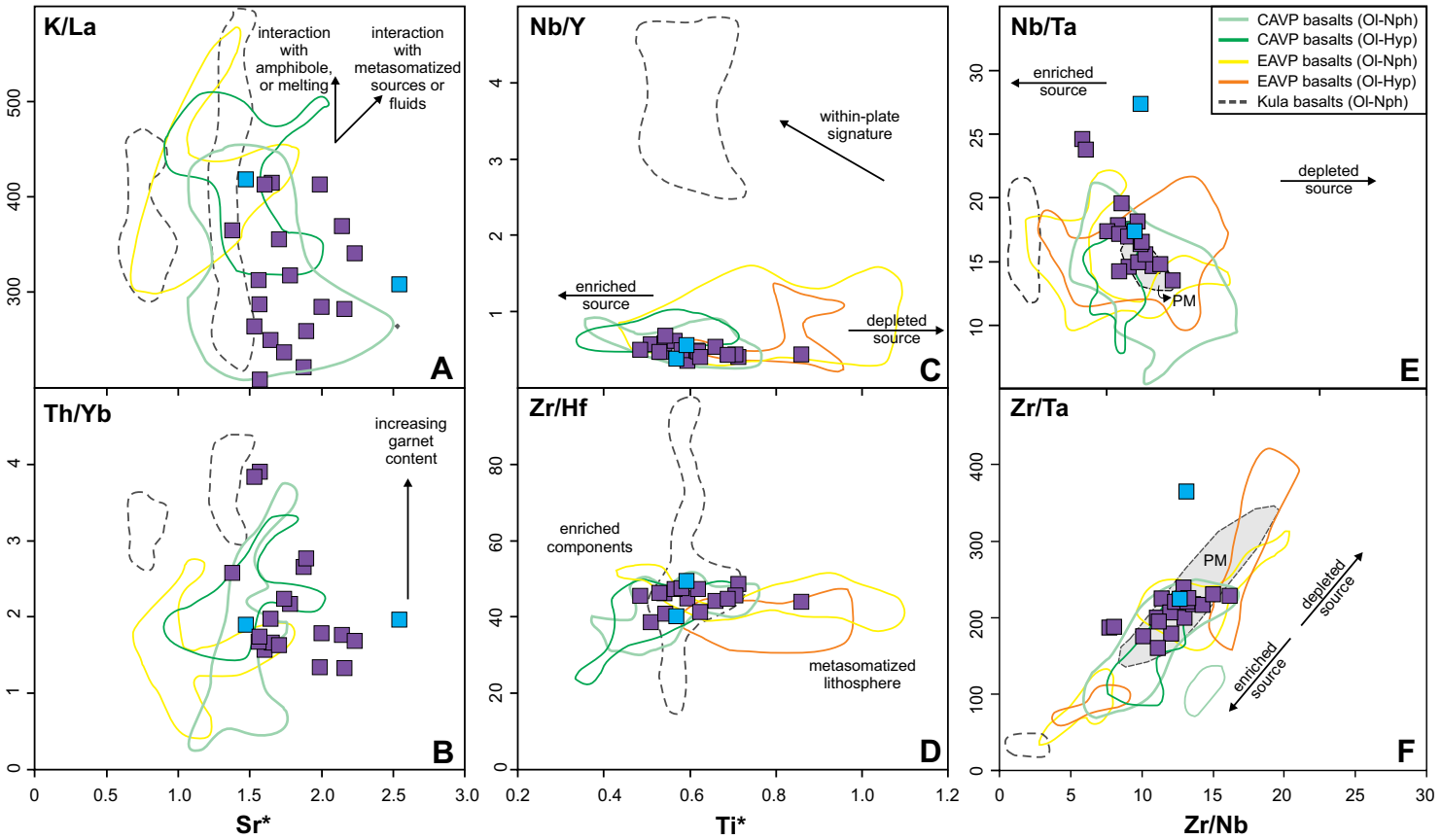

Figure 12. (A–B) Sr^*_N ($Sr_N/\sqrt{[Pr_N \times Nd_N]}$) vs. K/La and Th/Yb; (C–D) Ti^*_N ($Ti_N/\sqrt{[Pr_N \times Nd_N]}$) vs. Nb/Y and Zr/Hf; (E–F) Zr/Nb vs. Nb/Ta and Zr/Ta. See text for the references for Anatolian basalts. Primitive mantle (PM) composition is from Sun and McDonough (1989) and Palme and O'Neill (2003). CAVP—Central Anatolian volcanic province; EAVP—Eastern Anatolian volcanic province; Ol-Nph—olivine-nepheline; Ol-Hyp—olivine-hypersthene.

Possible Mantle Source Agents for Eğrikuyu Monogenetic Field Basalts

In Figure 13, we modified the diagrams proposed by Klaver et al. (2016) to show an incongruent batch melting model for Aegean arc basalts with a contribution from Eastern Mediterranean Sea sediments in their evolution. Th/Nb and Nb/Yb ratios are also important proxies for understanding enrichment by subduction or other processes (Pearce, 2008). The Eğrikuyu monogenetic field and Central Anatolian volcanic province basalts have elevated Th/Yb with Nb/Yb ratios, suggesting subduction-zone enrichment (Fig. 13A). Likewise, mixing of lower-degree melting (2%–6%) of subslab enriched mantle (SSEM) and higher-degree melting of average depleted mantle (ADM) with a contribution from Eastern Mediterranean Sea sediments (≥0.5) may explain the trace-element characteristics of the Eğrikuyu monogenetic field and Central Anatolian volcanic province basalts (Figs. 13A and 13B). Klaver et al. (2016) derived the SSEM composition assuming that Kula basalt (sample 26-wav of Chakrabarti et al., 2012) is consistent with 2% partial melting of a lherzolitic mantle that almost represents the subslab African lithospheric mantle. The ADM composition, on the other hand, is based on the depleted MORB mantle of Workman and Hart (2005), which was slightly modified by Klaver et al. (2016) (increased Zr and Hf contents). Details about the melting model and sediment contribution to the mixed source can be found in the supplementary file of Klaver et al. (2016).

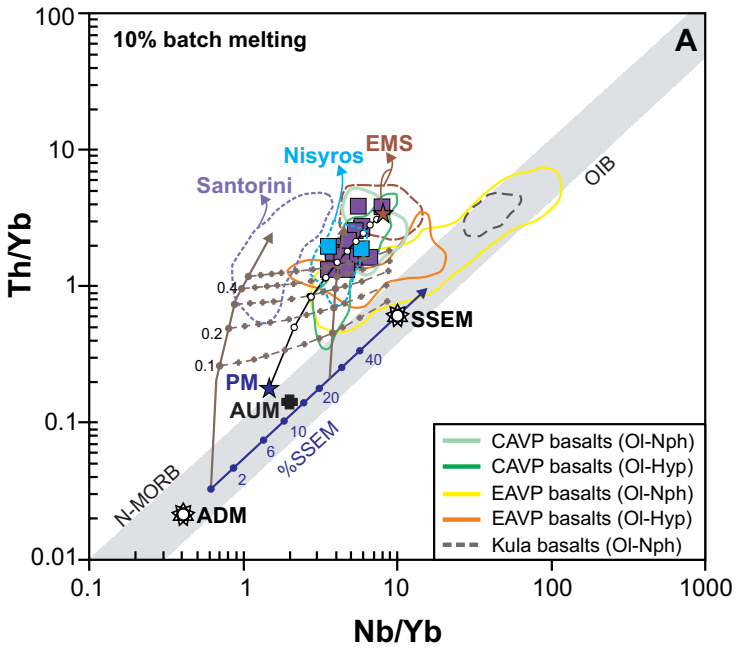

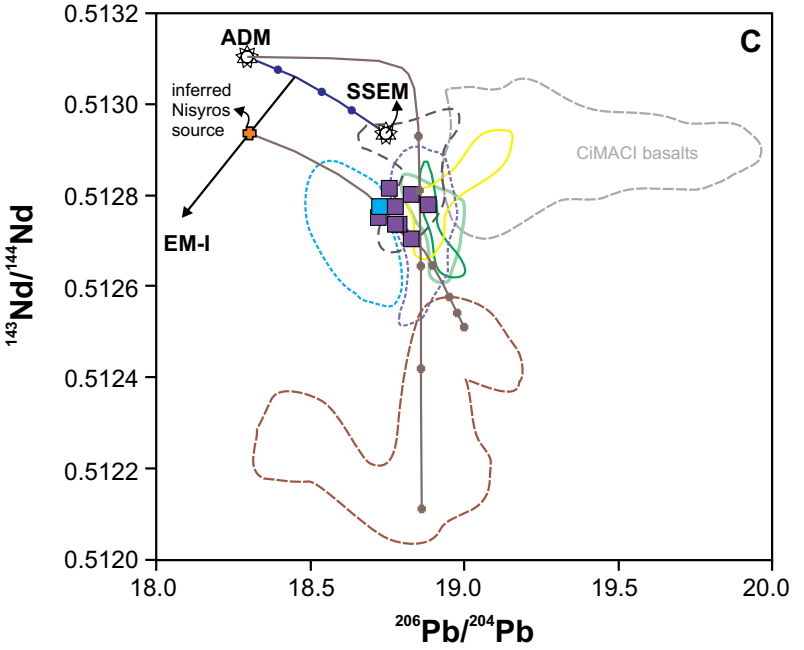

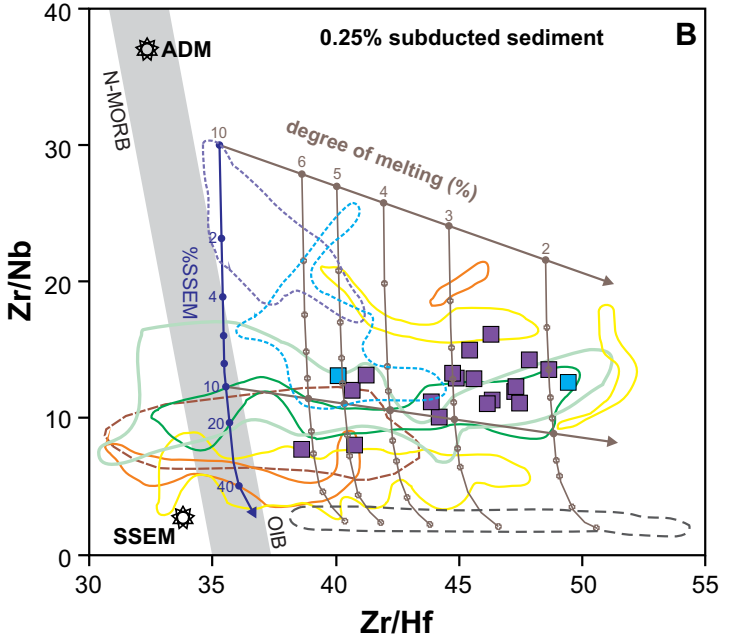

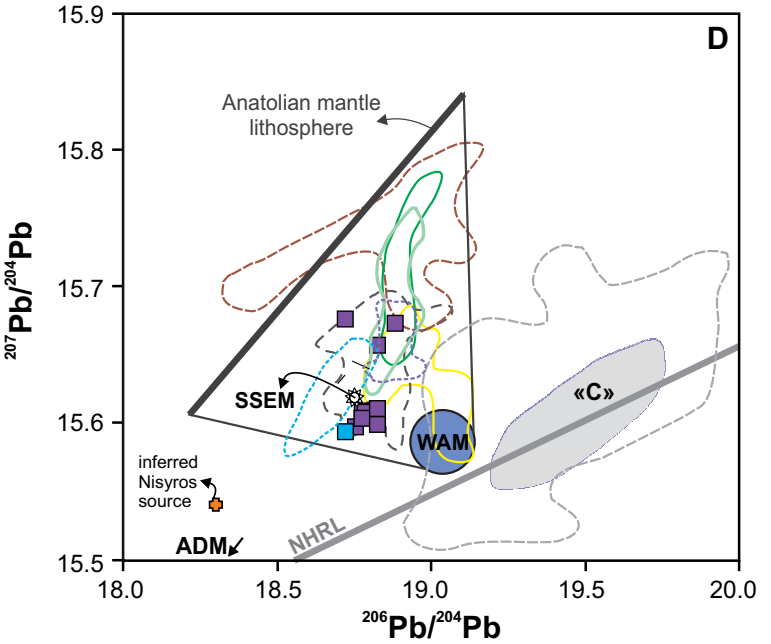

Figure 13. (A) Nb/Yb vs. Th/Yb. (B) Zr/Hf vs. Zr/Nb. (C–D) $^{206}Pb/^{204}Pb$ vs. $^{143}Nd/^{144}Nd$ and $^{207}Pb/^{204}Pb$. Incongruent batch melting model and Eastern Mediterranean Sea (EMS) sediment contribution lines between average depleted mantle (ADM) and subslab enriched mantle (SSEM) compositions are from Klaver et al. (2016). See text for the references for Anatolian and Aegean (Nisyros, Santorini) basalts. Subduction-modified mantle (SMM) and Central Anatolia ambient upper mantle (AUM) components are from Reid et al. (2017). CAVP—Central Anatolian volcanic province; EAVP—Eastern Anatolian volcanic province; Ol-Nph—olivine-nepheline; Ol-Hyp—olivine-hypersthene; OIB—oceanic-island basalt; N-MORB—normal mid-ocean-ridge basalt; PM—primitive mantle; EM-I—enriched mantle type 1; CiMACI—circum-Mediterranean anorogenic Cenozoic igneous basalts; "C"—"Common" mantle from Hanan and Graham (1996); NHRL—Northern Hemisphere reference line (Hart, 1984); WAM—western Anatolian mantle (Aldanmaz et al., 2015).

The trace-element characteristics of Eğrikuyu monogenetic field basalts mostly resemble those of Nisyros basalts, which can be derived from 4% partial melting of an enriched source, including 9% SSEM component with the addition of 0.15% Eastern Mediterranean Sea sediments (~0.15; Figs. 13A and 13B). The observed linear array in Figure 13B may indicate the continuity between the higher-degree melting of the ADM and lower-degree melting of the SSEM components. Contrary to the similarity in trace-element characteristics of the Eğrikuyu monogenetic field and Nisyros basalts, isotope compositions are not correlated, particularly in terms of $^{207}Pb/^{204}Pb$ (Figs. 13C and 13D). The inferred source for the Nisyros basalts that have enriched mantle type 1 (EM-I) affinity, representing the subcontinental lithospheric mantle of the African continent (Klaver et al., 2016), can partly explain the isotope composition of the Eğrikuyu monogenetic field basalts, with a lower contribution from Eastern Mediterranean Sea sediments (Fig. 13C). However, the Eğrikuyu monogenetic field basalts have distinct $^{207}Pb/^{204}Pb$ contents that are comparable to some Kula basalts (also comparable to the western Anatolian mantle "WAM" of Aldanmaz, 2002; Aldanmaz et al., 2006, 2015). Most of the Eğrikuyu monogenetic field basalts are clearly distinct from other Central Anatolian volcanic province basalts (Reid et al., 2017) that have elevated $^{207}Pb/^{204}Pb$ contents (Fig. 13D). Therefore, an inferred Nisyros source with any contribution of Eastern Mediterranean Sea sediments cannot form lower $^{207}Pb/^{204}Pb$ ratios, as seen in the Eğrikuyu monogenetic field basalts presented in this study (Fig. 13D).

Considering the trace-element and isotope characteristics of Eğrikuyu monogenetic field and Central Anatolian volcanic province basalts compared to Eastern Anatolian volcanic province and Kula basalts, we agree with the proposed SMM, AUM, and IPC components (Reid et al., 2017) for the generation of Eğrikuyu monogenetic field and Central Anatolian volcanic province basalts. Trace-element fingerprints of SMM (high La/Sm and Nb/Ta ratios) and AUM (low La/Sm and Nb/Ta ratios) components were also detected (Table 3; Fig. 12E). Pressure-dependent variations (not shown), especially in TiO_2 (0.79–1.51 wt%), Zr/Hf (38.6–49.4), and Ba/Nb (23.4–56.9), also support a contribution of IPC to the generation of the Eğrikuyu monogenetic field basalts. Moreover, Reid et al. (2017) stated that isotopic covariations (e.g., lower $^{207}Pb/^{204}Pb$) between Central Anatolian volcanic province basalts (mainly the Eğrikuyu monogenetic field) and IPC could not be demonstrated owing to the stronger imprint of mixed AUM-SMM arrays. However, the lower $^{207}Pb/^{204}Pb$ contents of our samples (except the three that have an SMM-dominated source) possibly represent the missing IPC signature of Reid et al. (2017). Therefore, it can be proposed that trace-element signature derived from IPC is diluted by enriched AUM + SMM, whereas their distinct isotopic signatures are still preserved in some of the Eğrikuyu monogenetic field basalts (Fig. 13D). Plotting of these Eğrikuyu monogenetic field basalts together with some of the Kula basalts (Alıcı et al., 2002; Chakrabarti et al., 2012; Aldanmaz et al., 2015) and Eastern Anatolian volcanic province basalts (Ekici et al., 2014) on isotope diagrams (Figs. 11C and 13D) also supports this interpretation.

In addition, traces of these components can also be followed in various mineral compositions (especially Ol and Cpx) of Eğrikuyu monogenetic field basalts. For instance, some of the Cpx compositions (including both ferroan and ferrian diopside) resemble alkali basalts derived from heterogeneous mantle sources (e.g., Duda and Schmincke, 1985; Albert et al., 2015; Jankovics et al., 2015). In particular, the presence of titanian augite and ferrian diopsides in the Eğrikuyu monogenetic field basalts might also reflect the presence of IPC in their sources.

Geodynamic Implications of Quaternary Volcanism in the Central Anatolian Volcanic Province

The recent geodynamic models, which are mainly based on geophysical and some petrological studies (e.g., Bartol and Govers, 2014; Delph et al., 2017; Reid et al., 2017; Schleiffarth et al., 2018), have provided new insight into the understanding of widespread volcanism in the Central Anatolian volcanic province. However, there are some contradictory interpretations (i.e., SW younging of Central Anatolian volcanism, a contribution from a deep-hot asthenosphere in the geochemistry of Central Anatolian volcanic province basalts) that the results from this study may help to clarify.

Volcanism in Central Anatolia (sensu lato) was initiated in the Late Cretaceous (ca. 76 Ma, Galatian volcanic province; Wilson et al., 1997; Koçyiğit et al., 2003, and references therein) during the closure of the northern Neo-Tethys ocean along the İzmir-Ankara-Erzincan suture zone and Inner Tauride suture zone (Fig. 1A). After the initiation of collision along the Bitlis suture zone around the early Miocene (ca. 23 Ma; Okay et al., 2010), volcanism continued in the Galatia volcanic province (ca. 19–10 Ma; Wilson et al., 1997; Varol et al., 2014), and also initiated in the western (Karacadağ, ca. 21–14 Ma; Asan and Kurt, 2011), southwestern (Erenlerdağ-Alacadağ-Sulutaş, ca. 22–3 Ma; Keller et al., 1977; Temel et al., 1998; Gençoğlu-Korkmaz et al., 2017), and eastern (Sivas volcanics, ca. 23–4 Ma; Platzman et al., 1998; Kürkçüoğlu et al., 2015; Kocaarslan and Ersoy, 2018) parts of the Kırşehir block (Fig. 1A). The start of Central Anatolian volcanic province volcanism, on the other hand, has been interpreted as late Miocene (ca. 13 Ma; Besang et al., 1977), and volcanism has continued until historical times (e.g., Schmitt et al., 2014). Considering all available information, it can be deduced that there is no clear evidence of a migration in time and space throughout Central Anatolia (cf. Schleiffarth et al., 2018). This is also supported by the disparate patterns of volcanism, even in the small monogenetic fields (Table 1; e.g., Eğrikuyu monogenetic field, 0.07–2.57 Ma; Notsu et al., 1995; Reid et al., 2017). However, while the lack of clear volcanic migration cannot totally reject recently proposed geodynamical models (e.g., Delph et al., 2017), the timing of slab rollback and break-off should be reconsidered.

Contrary to the OIB-like affinity of basalts in Galatia (ca. 10 Ma to Pliocene?; Wilson et al., 1997; Varol et al., 2014) and Sivas (especially Pliocene; Kürkçüoğlu et al., 2015; Kocaarslan and Ersoy, 2018), Central Anatolian volcanic province basalts (including mildly alkaline ones) have strong arc-type trace-element

patterns in the multi-element diagram (Fig. 10), probably due to melting of heterogeneous mantle sources (enriched lithosphere with a contribution from asthenosphere e.g., Gençalioğlu-Kuşcu and Geneli, 2010; Reid et al., 2017). The main strike-slip fault zones and related normal faults behaved as pathways for the Galatia and Sivas basalts, which have been interpreted to be derived from the asthenosphere, while there is a more complex geodynamic scenario for widespread volcanism in the Central Anatolian volcanic province (drip-like tectonism?; Reid et al., 2017; Göğüş et al., 2017). The alignment of volcanoes in the Central Anatolian volcanic province parallel to the Ecemiş fault zone and Tuz Gölü fault zone also indicates the role of tectonism in volcanism, but there is no clear evidence of an OIB-like asthenospheric source in the geochemical characteristics of Central Anatolian volcanics (e.g., Gençalioğlu-Kuşcu and Geneli, 2010, and references therein). Therefore, we totally disagree with some attempts (e.g., Aydin, 2008; Güçtekin and Köprübaşı, 2009) that suggest an OIB-like geochemical affinity for recent volcanics in the Central Anatolian volcanic province and a transition from orogenic to anorogenic magmatism, as in the case of many CiMACI provinces (Lustrino and Wilson, 2007). However, geochemical fingerprints of deep-hot upwelling asthenosphere (IPC of Reid et al., 2017) in the Central Anatolian volcanic province volcanics are only observed in some trace-element ratios (e.g., Ba/Nb, Zr/Hf; Reid et al., 2017), as well as lower $^{207}Pb/^{204}Pb$ ratios and distinct mineral compositions (e.g., titanian augite and ferrian diopsides) of Eğrikuyu monogenetic field basalts presented in this study (Figs. 8 and 11).

All these indications call into question whether Eğrikuyu monogenetic field basalts were derived from IPC or from a depleted part of an AUM component. In this case, the geodynamic model for the mid-Miocene to Pliocene Eastern Anatolian volcanics (Keskin, 2007) can be a good proxy for better understanding of the geochemical and geodynamic implications of Central Anatolian volcanic province basalts. Upwelling of asthenosphere through a slab tear (Gans et al., 2009; Biryol et al., 2011; Reid et al., 2017; Delph et al., 2017; Abgarmi et al., 2017) has been mainly characterized by low seismic velocities (Gans et al., 2009; Biryol et al., 2011; Delph et al., 2017; Abgarmi et al., 2017). However, as opposed to Quaternary Karacadağ basalts (Eastern Anatolian volcanic province; e.g., Lustrino et al., 2012; Ekici et al., 2014), the geochemical characteristics of upwelling asthenosphere (i.e., IPC) are somehow chemically diluted due to the interaction with enriched, but isotopically depleted, Anatolian lithosphere ((Fig. 13D; Reid et al., 2017). If this is the case, then we may conclude that some portions of Eğrikuyu monogenetic field basalts (presented in this study) isotopically represent the deeper upwelling asthenosphere, similar to sources of the Kula and Karacadağ basalts (Fig. 13D). Alternatively, lower $^{207}Pb/^{204}Pb$ ratios of some of the Eğrikuyu monogenetic field basalts represent the depleted portion of AUM, and therefore the contribution of chemically diluted IPC may not be clearly observed (or even absent) in the geochemistry of Central Anatolian volcanic province basalts (Reid et al., 2017).

The similarity in Eğrikuyu monogenetic field and Kula basalts in terms of isotope compositions is especially clear in Figure 13D, where some of the Eğrikuyu monogenetic field basalts are plotted close to the "western Anatolian mantle" of Aldanmaz et al. (2015, and references therein). On the other hand, possible reasons for the difference in trace-element characteristics between Eğrikuyu monogenetic field (i.e., arc-like signature with strong subduction enrichment) and Kula basalts (i.e., OIB-like with minor subduction enrichment) could be the different thicknesses of subduction-modified Anatolian lithosphere beneath western (i.e., thin) and central (i.e., relatively thick) Anatolia, differences in length, depth, and location of tears/break-off (Biryol et al., 2011) with respect to the basaltic field (e.g., Aegean vs. Kula basalts; Klaver et al., 2016), and the possible existence of drip tectonism in central Anatolia (Göğüş et al., 2017; Reid et al., 2017). In addition, the role of the Anatolian lithosphere is displayed in the Eastern Anatolian volcanic province basalts (except Karacadağ; e.g., Oyan et al., 2016, and references therein), which are similar to Eğrikuyu monogenetic field basalts in terms of both trace-element and isotope geochemistry (Figs. 11 and 13). Therefore, considering the initiation of the volcanism (ca. 13 Ma; Innocenti et al., 1976; Besang et al., 1977) and some similarities in the geochemical (i.e., existence of both primitive Ol-Hyp and Ol-Nph normative basalts, except for the OIB-like signature in some of the Eastern Anatolian volcanic province basalts; cf. Reid et al., 2017) and geodynamic (Keskin, 2007; Delph et al., 2017) characteristics of Central Anatolian and Eastern Anatolian volcanic province basalts, the idea of a single-slab delamination model proposed by Bartol and Govers (2014) should not be completely neglected.

CONCLUDING REMARKS

Eğrikuyu monogenetic field is one of the best examples of a monogenetic basaltic field in Anatolia in terms of not only spectacular morphology of the scoria cones and maars, but also petrological and geochemical diversity. The Eğrikuyu monogenetic field basalts are composed mainly of olivine ($Fo_{64–90}$) phenocrysts with clinopyroxene (mainly ferroan diopside with subordinate titanian augite and ferrian diopside) and plagioclase (labradorite to bytownite) microphenocrysts. They are mostly Ol-Nph normative alkali-olivine basalts (maximum normative Nph = 5.8%), but there are also two Ol-Hyp normative transitional basalts that are comparatively evolved (50–51 wt% SiO_2) relative to other basalts (45–50 wt% SiO_2), possibly owing to slight fractionation processes recognized in mafic mineral phases (mainly Ol plus minor Cpx). Eğrikuyu monogenetic field basalts are one of the most primitive basalts among the Quaternary Anatolian basalts, as shown by higher Mg# (63–72) and Ni (up to 226 ppm) contents. High LREE relative to HREE contents and a significant subduction signature on multi-element diagrams (depletion of Nb, Ta, P, and Ti) are diagnostic trace-element characteristics of the Eğrikuyu monogenetic field and other basalts in the Central Anatolian volcanic province.

Despite the similarity in multi-element patterns of all the Central Anatolian volcanic province basalts, there are at least two distinct source components in terms of mineral composition (e.g., including both ferroan and ferrian diopsides) and some trace-element (variable La/Sm, Nb/Ta, Zr/Hf, Th/Yb,

and Ba/Nb) and isotope ratios (lower $^{207}Pb/^{204}Pb$ only in some of the Eğrikuyu monogenetic field basalts). One of the distinct components is either deep-hot upwelling asthenosphere (IPC of Reid et al., 2017) through the Cyprian slab tear (Biryol et al., 2011), which is chemically enriched in the Eastern Mediterranean Sea sediment signature of Klaver et al. (2015), but isotopically depleted (lower $^{207}Pb/^{204}Pb$), or it was derived from an isotopically depleted portion of the AUM component (Reid et al., 2017). The other source component can be represented by subcontinental lithospheric mantle (SMM of Reid et al., 2017), which has been chemically and isotopically enriched by successive subduction events that have occurred in Central Anatolia since the Late Cretaceous. In addition, the high Nb/Ta ratios and depletion in Y and Yb observed in some of the Eğrikuyu monogenetic field basalts suggest a metasomatized enriched source that includes residual amphibole (plus rutile) and garnet.

Decompression melting (2%–6%) of mixed mantle components (with a greater proportion of SMM) may explain the diverse geochemical characteristics of the Eğrikuyu monogenetic field and other Central Anatolian volcanic province basalts. The small degree of crustal contamination and mafic mineral fractionation may also contribute to the trace-element compositions within these basalts. Most recent geophysical and geodynamical studies also have supported the existence of upwelling asthenosphere at shallow levels beneath Central Anatolia, and the Eğrikuyu monogenetic field is located within the region in the Central Anatolian volcanic province where low Pn velocity anomalies (Gans et al., 2009; Biryol et al., 2011) and also thinner crust (Abgarmi et al., 2017) are observed. Although it is geochemically difficult to constrain the geodynamic processes responsible for the evolution of the Central Anatolian volcanic province, a role can be proposed for deep, hot, and slightly enriched asthenospheric mantle that rose through a slab tear and interacted with either dripping (Reid et al., 2017; Göğüş et al., 2017) or overlying (Kadıoğlu and Dilek, 2010) previously enriched subcontinental lithospheric mantle. Alternatively, melting of mixed SMM and AUM components (Reid et al., 2017) triggered by lithospheric-scale transtensional fault systems in the Central Anatolian volcanic province could have formed the Central Anatolian volcanic province basalts without a contribution from the deep asthenospheric mantle (e.g., Gençalioğlu-Kuşcu and Geneli, 2010). Differences in the residence time of the Eğrikuyu monogenetic field basalts while rising to the surface can also explain the record of chemical heterogeneity (Gençalioğlu-Kuşcu and Geneli, 2010). Drip-tectonism (Göğüş et al., 2017) and crustal variations throughout the Central Anatolian volcanic province (Uluocak et al., 2016; Abgarmi et al., 2017) may have fostered uplift of the region. Therefore, rising of deep asthenosphere through a slab tear would not be required to explain the generation of volcanism in the Central Anatolian volcanic province.

Our findings indicate that the Eğrikuyu monogenetic field displays mantle source heterogeneity in Quaternary basalts of the Central Anatolian volcanic province, and it also represents a distinct mantle source isotopically similar to the western Anatolian mantle (WAM) of Aldanmaz et al. (2015). In addition, we reveal the importance of a detailed petrological investigation in a small monogenetic basaltic field with increased geochemical sampling.

ACKNOWLEDGMENTS

This study was the M.Sc. dissertation of G. Uslular, and it was supported by grants from the Scientific Research Projects of Muğla Sıtkı Koçman University (project numbers 13/95 and 15/211) and the "Continental Dynamics: Central Anatolian Tectonics (CD-CAT)" project funded by National Science Foundation (grant EAR 1109762 to Donna Whitney). We thank Mary R. Reid for supporting some parts of the field trips. We would like to thank Donna Whitney and Andreas Kronz for the mineral chemistry analyses. We also thank Serhat Köksal for the isotope analyses. Uslular is especially thankful to İlkay Kuşcu for his pertinent and helpful comments. We kindly acknowledge the editorial handling by Raymond M. Russo and Guest Associate Editor Christian Teyssier and also comments by Karoly Németh and one anonymous reviewer. Primitive versions (or templates before vector modifications) of the geochemical diagrams were drawn using GCDkit (Janoušek et al., 2006).

REFERENCES CITED

Abgarmi, B., Delph, J.R., Ozacar, A.A., Beck, S.L., Zandt, G., Sandvol, E., Türkelli, N., and Biryol, C.B., 2017, Structure of the crust and African slab beneath the Central Anatolian Plateau from receiver functions: New insights on isostatic compensation and slab dynamics: Geosphere, v. 13, no. 6, p. 1774–1787, https://doi.org/10.1130/GES01509.1.

Albert, H., Costa, F., and Martí, J., 2015, Timing of magmatic processes and unrest associated with mafic historical monogenetic eruptions in Tenerife Island: Journal of Petrology, v. 56, no. 10, p. 1945–1966, https://doi.org/10.1093/petrology/egv058.

Aldanmaz, E., 2002, Mantle source characteristics of alkali basalts and basanites in an extensional intracontinental plate setting, western Anatolia, Turkey: Implications for multi-stage melting: International Geology Review, v. 44, no. 5, p. 440–457, https://doi.org/10.2747/0020-6814.44.5.440.

Aldanmaz, E., Köprübaşı, N., Gürer, Ö.F., Kaymakçı, N., and Gourgaud, A., 2006, Geochemical constraints on the Cenozoic, OIB-type alkaline volcanic rocks of NW Turkey: Implications for mantle sources and melting processes: Lithos, v. 86, no. 1–2, p. 50–76, https://doi.org/10.1016/j.lithos.2005.04.003.

Aldanmaz, E., Pickard, M., Meisel, T., Altunkaynak, Ş., Sayıt, K., Şen, P., Hanan, B.B., and Furman, T., 2015, Source components and magmatic processes in the genesis of Miocene to Quaternary lavas in western Turkey: Constraints from HSE distribution and Hf-Pb-Os isotopes: Contributions to Mineralogy and Petrology, v. 170, no. 2, p. 23, https://doi.org/10.1007/s00410-015-1176-x.

Alıcı, P., Temel, A., and Gourgaud, A., 2002, Pb-Nd-Sr isotope and trace element geochemistry of Quaternary extension-related alkaline volcanism: A case study of Kula region (Western Anatolia, Turkey): Journal of Volcanology and Geothermal Research, v. 115, no. 3–4, p. 487–510, https://doi.org/10.1016/S0377-0273(01)00328-6.

Alıcı-Şen, P., Temel, A., and Gourgaud, A., 2004, Petrogenetic modelling of Quaternary post-collisional volcanism: A case study of Central and Eastern Anatolia: Geological Magazine, v. 141, no. 1, p. 81–98, https://doi.org/10.1017/S0016756803008550.

Arcasoy, A., 2001, A New Method for Detecting the Alignments from Point-Like Features: An Application to the Volcanic Cones of Cappadocian Volcanic Province, Turkey [Ph.D. thesis]: Ankara, Turkey, Middle East Technical University, 157 p.

Asan, K., and Kurt, H., 2011, Petrology and geochemistry of post-collisional early Miocene volcanism in the Karacadağ area (Central Anatolia, Turkey): Acta Geologica Sinica [English Edition], v. 85, no. 5, p. 1100–1117, https://doi.org/10.1111/j.1755-6724.2011.00543.x.

Ateş, A., Bilim, F., and Büyüksaraç, A., 2005, Curie point depth investigation of Central Anatolia, Turkey: Pure and Applied Geophysics, v. 162, no. 2, p. 357–371, https://doi.org/10.1007/s00024-004-2605-3.

Aydar, E., and Gourgaud, A., 1998, The geology of Mount Hasan stratovolcano, central Anatolia, Turkey: Journal of Volcanology and Geothermal Research, v. 85, no. 1–4, p. 129–152, https://doi.org/10.1016/S0377-0273(98)00053-5.

Aydar, E., Gourgaud, A., Deniel, C., Lyberis, N., and Gündoğdu, N., 1995, Le volcanisme quaternaire d'Anatolie centrale (Turquie): Association de magmatismes calco-alcalin et alcalin en domaine de convergence: Canadian Journal of Earth Sciences, v. 32, no. 7, p. 1058–1069, https://doi.org/10.1139/e95-087.

Aydin, F., 2008, Contrasting complexities in the evolution of calc-alkaline and alkaline melts of the Niğde volcanic rocks, Turkey: Textural, mineral chemical and geochemical evidence:

European Journal of Mineralogy, v. 20, no. 1, p. 101–118, https://doi.org/10.1127/0935-1221/2008/0020-1784.
Aydin, F., Schmitt, A.K., Siebel, W., Sönmez, M., Ersoy, Y., Lermi, A., Dirik, K., and Duncan, R., 2014, Quaternary bimodal volcanism in the Niğde volcanic complex (Cappadocia, Central Anatolia, Turkey): Age, petrogenesis and geodynamic implications: Contributions to Mineralogy and Petrology, v. 168, no. 5, p. 1078, https://doi.org/10.1007/s00410-014-1078-3.
Báez, W., Nuñez, G.C., Giordano, G., Viramonte, J.G., and Chiodi, A., 2017, Polycyclic scoria cones of the Antofagasta de la Sierra basin, Southern Puna plateau, Argentina, *in* Németh, K., Carrasco-Núñez, G., Aranda-Gómez, J.J., and Smith, I.E.M., eds., Monogenetic Volcanism: Geological Society, London, Special Publication 446, p. 311–336, https://doi.org/10.1144/SP446.3.
Bailey, J.C., Jensen, E.S., Hansen, A., Kann, A.D.J., and Kann, K., 2009, Formation of heterogeneous magmatic series beneath North Santorini, South Aegean island arc: Lithos, v. 110, no. 1, p. 20–36, https://doi.org/10.1016/j.lithos.2008.12.002.
Bartol, J., and Govers, R., 2014, A single cause for uplift of the Central and Eastern Anatolian Plateau?: Tectonophysics, v. 637, p. 116–136, https://doi.org/10.1016/j.tecto.2014.10.002.
Batum, İ., 1978, Nevşehir güneybatısındaki Göllüdağ ve Acıgöl yöresi volkanitlerinin jeoloji ve petrografisi: Yerbilimleri Dergisi (Earth Sciences), v. 5, no. 3/4, p. 50–69 [in Turkish].
Bayer-Altın, T., El Ouahabi, M., and Fagel, N., 2015, Environmental and climatic changes during the Pleistocene–Holocene in the Bor Plain, Central Anatolia, Turkey: Palaeogeography, Palaeoclimatology, Palaeoecology, v. 440, p. 564–578, https://doi.org/10.1016/j.palaeo.2015.09.011.
Bellieni, G., Justin Visentin, E., Le Maitre, R.W., Piccirillo, E.M., and Zanettin, B., 1983, Proposal for a Division of the Basaltic (B) Field of the TAS Diagram: International Union of Geological Sciences (IUGS) Subcommission on the Systematics of Igneous Rocks Circular 38, Contribution 102.
Besang, C., Eckhardt, F.J., Harre, W., Kreuzer, H., and Müller, P., 1977, Radiometrische altersbestimmungen an Neogenen eruptivgesteinen der Türkei: Geologisches Jahrbuch, v. 25, p. 3–36.
Biryol, B.C., Beck, S.L., Zandt, G., and Özacar, A.A., 2011, Segmented African lithosphere beneath the Anatolian region inferred from teleseismic P-wave tomography: Geophysical Journal International, v. 184, no. 3, p. 1037–1057, https://doi.org/10.1111/j.1365-246X.2010.04910.x.
Brenna, M., Cronin, S.J., Smith, I.E., Sohn, Y.K., and Németh, K., 2010, Mechanisms driving polymagmatic activity at a monogenetic volcano, Udo, Jeju Island, South Korea: Contributions to Mineralogy and Petrology, v. 160, no. 6, p. 931–950, https://doi.org/10.1007/s00410-010-0515-1.
Buettner, A., Kleinhanns, I.C., Rufer, D., Hunziker, J.C., and Villa, I.M., 2005, Magma generation at the easternmost section of the Hellenic arc: Hf, Nd, Pb and Sr isotope geochemistry of Nisyros and Yali volcanoes (Greece): Lithos, v. 83, no. 1–2, p. 29–46, https://doi.org/10.1016/j.lithos.2005.01.001.
Chakrabarti, R., Basu, A.R., and Ghatak, A., 2012, Chemical geodynamics of Western Anatolia: International Geology Review, v. 54, no. 2, p. 227–248, https://doi.org/10.1080/00206814.2010.543787.
Connor, C.B., and Conway, F.M., 2000, Basaltic volcanic fields, *in* Sigurdsson, H., ed., Encyclopedia of Volcanoes: New York, Academic Press, p. 331–343.
Cosentino, D., Schildgen, T.F., Cipollari, P., Faranda, C., Gliozzi, E., Hudáčková, N., Lucifora, S., and Strecker, M.R., 2012, Late Miocene surface uplift of the southern margin of the Central Anatolian Plateau, Central Taurides, Turkey: Geological Society of America Bulletin, v. 124, no. 1–2, p. 133–145, https://doi.org/10.1130/B30466.1.
Delph, J.R., Abgarmi, B., Ward, K.M., Beck, S.L., Özacar, A.A., Zandt, G., Sandvol, E., Türkelli, N., and Kalafat, D., 2017, The effects of subduction termination on the continental lithosphere: Linking volcanism, deformation, surface uplift, and slab tearing in Central Anatolia: Geosphere, v. 13, no. 6, p. 1788–1805, https://doi.org/10.1130/GES01478.1.
Deniel, C., Aydar, E., and Gourgaud, A., 1998, The Hasan Dağı stratovolcano (Central Anatolia, Turkey): Evolution from calc-alkaline to alkaline magmatism in a collision zone: Journal of Volcanology and Geothermal Research, v. 87, no. 1–4, p. 275–302, https://doi.org/10.1016/S0377-0273(98)00097-3.
DePaolo, D.J., and Daley, E.E., 2000, Neodymium isotopes in basalts of the southwest Basin and Range and lithospheric thinning during continental extension: Chemical Geology, v. 169, no. 1–2, p. 157–185, https://doi.org/10.1016/S0009-2541(00)00261-8.
Doğan-Külahçı, G.D., Temel, A., Gourgaud, A., Varol, E., Guillou, H., and Deniel, C., 2018, Contemporaneous alkaline and calc-alkaline series in Central Anatolia (Turkey): Spatio-temporal evolution of a post-collisional Quaternary basaltic volcanism: Journal of Volcanology and Geothermal Research, v. 356, p. 56–74, https://doi.org/10.1016/j.jvolgeores.2018.02.012.
Druitt, T.H., Brenchley, P.J., Gökten, Y.E., and Francaviglia, V., 1995, Late Quaternary rhyolitic eruptions from the Acigöl complex, central Turkey: Journal of the Geological Society [London], v. 152, no. 4, p. 655–667, https://doi.org/10.1144/gsjgs.152.4.0655.
Duda, A., and Schmincke, H.U., 1985, Polybaric differentiation of alkali basaltic magmas: Evidence from green-core clinopyroxenes (Eifel, FRG): Contributions to Mineralogy and Petrology, v. 91, no. 4, p. 340–353, https://doi.org/10.1007/BF00374690.
Ekici, T., Macpherson, C.G., and Otlu, N., 2012, Polybaric melting of a single mantle source during the Neogene Siverek phase of the Karacadağ volcanic complex, SE Turkey: Lithos, v. 146–147, p. 152–163, https://doi.org/10.1016/j.lithos.2012.05.004.
Ekici, T., Macpherson, C.G., Otlu, N., and Fontignie, D., 2014, Foreland magmatism during the Arabia-Eurasia collision: Pliocene–Quaternary activity of the Karacadağ volcanic complex, SW Turkey: Journal of Petrology, v. 55, no. 9, p. 1753–1777, https://doi.org/10.1093/petrology/egu040.
Ercan, T., 1993, Interpretation of geochemical, radiometric and isotopic data on Kula volcanics (Manisa-W. Anatolia): Geological Bulletin of Turkey, v. 36, p. 113–129.
Ercan, T., Tokel, S., Matsuda, J.I., Ul, T., Notsu, K., and Fujitani, T., 1992, New geochemical, isotopic and radiometric data of the Quaternary volcanism of Hasandağı-Karacadağ (Central Anatolia): Türkiye Jeoloji Bülteni, v. 7, p. 8–21 [in Turkish].
Ersoy, Y.E., Helvacı, C., and Palmer, M.R., 2012, Petrogenesis of the Neogene volcanic units in the NE-SW–trending basins in Western Anatolia, Turkey: Contributions to Mineralogy and Petrology, v. 163, no. 3, p. 379–401, https://doi.org/10.1007/s00410-011-0679-3.
Foley, S., Venturelli, G., Green, D.H., and Toscani, L., 1987, The ultrapotassic rocks: Characteristics, classification, and constraints for petrogenetic models: Earth-Science Reviews, v. 24, no. 2, p. 81–134, https://doi.org/10.1016/0012-8252(87)90001-8.
Gall, H., Furman, D., Kürkçüoğlu, B., and Pickard, M., 2014, Origin of mafic lavas at Hasandağ stratovolcano, Central Anatolian volcanic zone: Geological Society of America Abstracts with Programs, v. 46, no. 6, abstract 224–17.
Gans, C.R., Beck, S.L., Zandt, G., Biryol, C.B., and Özacar, A.A., 2009, Detecting the limit of slab break-off in central Turkey: New high-resolution Pn tomography results: Geophysical Journal International, v. 179, no. 3, p. 1566–1572, https://doi.org/10.1111/j.1365-246X.2009.04389.x.
Genç, Y., and Yürür, M.T., 2010, Coeval extension and compression in late Mesozoic–Recent thin-skinned extensional tectonics in Central Anatolia, Turkey: Journal of Structural Geology, v. 32, no. 5, p. 623–640, https://doi.org/10.1016/j.jsg.2010.03.011.
Gençalioğlu-Kuşcu, G., 2011, Geochemical characterization of a Quaternary monogenetic volcano in Erciyes volcanic complex: Cora Maar (Central Anatolian volcanic province, Turkey): International Journal of Earth Sciences, v. 100, no. 8, p. 1967–1985, https://doi.org/10.1007/s00531-010-0620-4.
Gençalioğlu-Kuşcu, G., and Geneli, F., 2010, Review of post-collisional volcanism in the Central Anatolian volcanic province (Turkey), with special reference to the Tepeköy volcanic complex: International Journal of Earth Sciences, v. 99, no. 3, p. 593–621, https://doi.org/10.1007/s00531-008-0402-4.
Gençalioğlu-Kuşcu, G., Atilla, C., Cas, R.A., and Kuşcu, İ., 2007, Base surge deposits, eruption history, and depositional processes of a wet phreatomagmatic volcano in Central Anatolia (Cora Maar): Journal of Volcanology and Geothermal Research, v. 159, no. 1–3, p. 198–209, https://doi.org/10.1016/j.jvolgeores.2006.06.013.
Gençoğlu-Korkmaz, G., Asan, K., Kurt, H., and Morgan, G., 2017, $^{40}Ar/^{39}Ar$ geochronology, elemental and Sr-Nd-Pb isotope geochemistry of the Neogene bimodal volcanism in the Yükselen area, NW Konya (Central Anatolia, Turkey): Journal of African Earth Sciences, v. 129, p. 427–444, https://doi.org/10.1016/j.jafrearsci.2017.02.001.
Gill, R., 2010, Igneous Rocks and Processes: A Practical Guide: Oxford, UK, John Wiley & Sons, 428 p.
Göğüş, O.H., Pysklywec, R.N., Şengör, A.M.C., and Gün, E., 2017, Drip tectonics and the enigmatic uplift of the Central Anatolian Plateau: Nature Communications, v. 8, no. 1, p. 1538, https://doi.org/10.1038/s41467-017-01611-3.
Görür, N., Oktay, F.Y., Seymen, İ., and Şengör, A.M.C., 1984, Palaeotectonic evolution of the Tuzgölü basin complex, central Turkey: Sedimentary record of a Neo-Tethyan closure, *in* Dixon, J.E., and Robertson, A.H.F., eds., Geological Evolution of the Eastern Mediterranean: Geological Society, London, Special Publication 17, p. 467–482.

Grützner, T., Prelević, D., and Akal, C., 2013, Geochemistry and origin of ultramafic enclaves and their basanitic host rock from Kula volcano, Turkey: Lithos, v. 180–181, p. 58–73, https://doi.org/10.1016/j.lithos.2013.08.001.

Güçtekin, A., and Köprübaşı, N., 2009, Geochemical characteristics of mafic and intermediate volcanic rocks from the Hasandağ and Erciyes volcanoes (Central Anatolia, Turkey): Turkish Journal of Earth Sciences, v. 18, no. 1, p. 1–27.

Hanan, B.B., and Graham, D.W., 1996, Lead and helium isotope evidence from oceanic basalts for a common deep source of mantle plumes: Science, v. 272, p. 991–995, https://doi.org/10.1126/science.272.5264.991.

Harangi, S., Jankovics, M.É., Sági, T., Kiss, B., Lukács, R., and Soós, I., 2015, Origin and geodynamic relationships of the late Miocene to Quaternary alkaline basalt volcanism in the Pannonian basin, eastern-central Europe: International Journal of Earth Sciences, v. 104, no. 8, p. 2007–2032, https://doi.org/10.1007/s00531-014-1105-7.

Hart, S.R., 1984, A large-scale isotope anomaly in the Southern Hemisphere mantle: Nature, v. 309, no. 5971, p. 753–757, https://doi.org/10.1038/309753a0.

Hirose, K., and Kushiro, I., 1993, Partial melting of dry peridotites at high pressures: Determination of compositions of melts segregated from peridotite using aggregates of diamond: Earth and Planetary Science Letters, v. 114, no. 4, p. 477–489, https://doi.org/10.1016/0012-821X(93)90077-M.

Innocenti, F., Mazzuoli, R., Pasquare, G., Di Brozolo, F.R., and Villari, L., 1976, Evolution of the volcanism in the area of interaction between the Arabian, Anatolian and Iranian plates (Lake Van, eastern Turkey): Journal of Volcanology and Geothermal Research, v. 1, no. 2, p. 103–112, https://doi.org/10.1016/0377-0273(76)90001-9.

Innocenti, F., Agostini, S., Di Vincenzo, G., Doglioni, C., Manetti, P., Savaşçın, M.Y., and Tonarini, S., 2005, Neogene and Quaternary volcanism in Western Anatolia: Magma sources and geodynamic evolution: Marine Geology, v. 221, no. 1–4, p. 397–421, https://doi.org/10.1016/j.margeo.2005.03.016.

Irvine, T.N.J., and Baragar, W.R.A.F., 1971, A guide to the chemical classification of the common volcanic rocks: Canadian Journal of Earth Sciences, v. 8, no. 5, p. 523–548, https://doi.org/10.1139/e71-055.

Jankovics, M.É., Harangi, S., Németh, K., Kiss, B., and Ntaflos, T., 2015, A complex magmatic system beneath the Kissomlyó monogenetic volcano (western Pannonian Basin): Evidence from mineral textures, zoning and chemistry: Journal of Volcanology and Geothermal Research, v. 301, p. 38–55, https://doi.org/10.1016/j.jvolgeores.2015.04.010.

Janoušek, V., Farrow, C.M., and Erban, V., 2006, Interpretation of whole-rock geochemical data in igneous geochemistry: Introducing Geochemical Data Toolkit (GCDkit): Journal of Petrology, v. 47, no. 6, p. 1255–1259, https://doi.org/10.1093/petrology/egl013.

Johannsen, A., 1931, A Descriptive Petrography of the Igneous Rocks: Volume 1. Introduction, Textures, Classifications and Glossary: Chicago, Illinois, University of Chicago Press, 267 p.

Kadıoğlu, Y.K., and Dilek, Y., 2010, Structure and geochemistry of the adakitic Horoz granitoid, Bolkar Mountains, south-central Turkey, and its tectonomagmatic evolution: International Geology Review, v. 52, no. 4–6, p. 505–535, https://doi.org/10.1080/09507110902954847.

Keller, J., 1974, Quaternary maar volcanism near Karapinar in Central Anatolia: Bulletin Volcanologique, v. 38, no. 1, p. 378–396, https://doi.org/10.1007/BF02599413.

Keller, J., Jung, D., Burgath, K., and Wolf, F., 1977, Geology and petrology of the Neogene calc-alcalic volcanic rocks in the Konya region (Erenler Dağ, Alaca Dağ Massif, Central Anatolia): Geologisches Jahrbuch, 25, p. 37–117 (in German).

Kereszturi, G., and Németh, K., 2012, Monogenetic basaltic volcanoes: Genetic classification, growth, geomorphology and degradation, *in* Németh, K., ed., Updates in Volcanology—New Advances in Understanding Volcanic System: InTech, p. 1–89, https://doi.org/10.5772/51387.

Keskin, M., 2007, Eastern Anatolia: A hotspot in a collision zone without a mantle plume, *in* Foulger, G.R., and Jurdy, D.M., eds., Plates, Plumes and Planetary Processes: Geological Society of America Special Paper 430, p. 693–722, https://doi.org/10.1130/2007.2430(32).

Klaver, M., Djuly, T., de Graaf, S., Sakes, A., Wijbrans, J., Davies, G., and Vroon, P., 2015, Temporal and spatial variations in provenance of Eastern Mediterranean Sea sediments: Implications for Aegean and Aeolian arc volcanism: Geochimica et Cosmochimica Acta, v. 153, p. 149–168, https://doi.org/10.1016/j.gca.2015.01.007.

Klaver, M., Davies, G.R., and Vroon, P.Z., 2016, Subslab mantle of African provenance infiltrating the Aegean mantle wedge: Geology, v. 44, no. 5, p. 367–370, https://doi.org/10.1130/G37627.1.

Kocaarslan, A., and Ersoy, E.Y., 2018, Petrologic evolution of Miocene–Pliocene mafic volcanism in the Kangal and Gürün basins (Sivas-Malatya), central east Anatolia: Evidence for Miocene anorogenic magmas contaminated by continental crust: Lithos, v. 310–311, p. 392–408, https://doi.org/10.1016/j.lithos.2018.04.021.

Koçyiğit, A., and Beyhan, A., 1998, A new intracontinental transcurrent structure: The Central Anatolian fault zone, Turkey: Tectonophysics, v. 284, no. 3–4, p. 317–336, https://doi.org/10.1016/S0040-1951(97)00176-5.

Koçyiğit, A., Winchester, J.A., Bozkurt, E., and Holland, G., 2003, Saraçköy volcanic suite: Implications for the subductional phase of arc evolution in the Galatean arc complex, Ankara, Turkey: Geological Journal, v. 38, no. 1, p. 1–14, https://doi.org/10.1002/gj.921.

Köksal, S., Toksoy-Köksal, F., and Göncüoglu, M.C., 2017, Petrogenesis and geodynamics of plagiogranites from Central Turkey (Ekecikdağ/Aksaray): New geochemical and isotopic data for generation in an arc basin system within the northern branch of Neotethys: International Journal of Earth Sciences, v. 106, no. 4, p. 1181–1203, https://doi.org/10.1007/s00531-016-1401-5.

Köprübaşı, N., Güçtekin, A., Çelebi, D., and Kırmacı, M.Z., 2014, Mineral chemical constraints on the petrogenesis of mafic and intermediate volcanic rocks from the Erciyes and Hasandağ volcanoes: Central Turkey: Chemie der Erde (Geochemistry), v. 74, no. 4, p. 585–600.

Kürkçüoğlu, B., 2010, Geochemistry and petrogenesis of basaltic rocks from the Develidağ volcanic complex, Central Anatolia, Turkey: Journal of Asian Earth Sciences, v. 37, no. 1, p. 42–51, https://doi.org/10.1016/j.jseaes.2009.07.004.

Kürkçüoğlu, B., Sen, E., Aydar, E., Gourgaud, A., and Gündogdu, N., 1998, Geochemical approach to magmatic evolution of Mt. Erciyes stratovolcano, Central Anatolia, Turkey: Journal of Volcanology and Geothermal Research, v. 85, no. 1–4, p. 473–494, https://doi.org/10.1016/S0377-0273(98)00067-5.

Kürkçüoğlu, B., Pickard, M., Şen, P., Hanan, B.B., Sayıt, K., Plummer, C., Şen, E., Yürür, T., and Furman, T., 2015, Geochemistry of mafic lavas from Sivas, Turkey and the evolution of Anatolian lithosphere: Lithos, v. 232, p. 229–241, https://doi.org/10.1016/j.lithos.2015.07.006.

Kuzucuoğlu, C., Pastre, J.F., Black, S., Ercan, T., Fontugne, M., Guillou, H., Hatte, C., Karabıyıkoğlu, M., Orth, P., and Türkecan, A., 1998, Identification and dating of tephra layers from Quaternary sedimentary sequences of Inner Anatolia, Turkey: Journal of Volcanology and Geothermal Research, v. 85, no. 1–4, p. 153–172, https://doi.org/10.1016/S0377-0273(98)00054-7.

Lebedev, V.A., Chugaev, A.V., Ünal, E., Sharkov, E.V., and Keskin, M., 2016, Late Pleistocene Tendürek volcano (Eastern Anatolia, Turkey). II. Geochemistry and petrogenesis of the rocks: Petrology, v. 24, no. 3, p. 234–270, https://doi.org/10.1134/S0869591116030048.

Lee, C.T.A., Luffi, P., Plank, T., Dalton, H., and Leeman, W.P., 2009, Constraints on the depths and temperatures of basaltic magma generation on Earth and other terrestrial planets using new thermobarometers for mafic magmas: Earth and Planetary Science Letters, v. 279, no. 1–2, p. 20–33, https://doi.org/10.1016/j.epsl.2008.12.020.

Le Maitre, R.W., Streckeisen, A., Zanettin, B., Le Bas, M.J., Bonin, B., Bateman, P., Bellieni, G., Dudek, A., Efremova, S., Keller, J., Lameyre, J., Sabine, P.A., Schmid, R., and Sorensen, H., 2002, Igneous Rocks: A Classification and Glossary of Terms; Recommendations of the International Union of Geological Sciences Subcommission on the Systematics of Igneous Rocks: Cambridge, UK, Cambridge University Press, 236 p., https://doi.org/10.1017/CBO9780511535581.

Leterrier, J., Maury, R.C., Thonon, P., Girard, D., and Marchal, M., 1982, Clinopyroxene composition as a method of identification of the magmatic affinities of paleo-volcanic series: Earth and Planetary Science Letters, v. 59, no. 1, p. 139–154, https://doi.org/10.1016/0012-821X(82)90122-4.

Luhr, J.F., Allan, J.F., Carmichael, I.S., Nelson, S.A., and Hasenaka, T., 1989, Primitive calc-alkaline and alkaline rock types from the Western Mexican volcanic belt: Journal of Geophysical Research–Solid Earth, v. 94, no. B4, p. 4515–4530, https://doi.org/10.1029/JB094iB04p04515.

Lustrino, M., and Dallai, L., 2003, On the origin of EM-I end-member: Neues Jahrbuch für Mineralogie, Abhandlungen, v. 179, no. 1, p. 85–100.

Lustrino, M., and Wilson, M., 2007, The circum-Mediterranean anorogenic Cenozoic igneous province: Earth-Science Reviews, v. 81, no. 1–2, p. 1–65, https://doi.org/10.1016/j.earscirev.2006.09.002.

Lustrino, M., Keskin, M., Mattioli, M., Lebedev, V.A., Chugaev, A., Sharkov, E., and Kavak, O., 2010, Early activity of the largest Cenozoic shield volcano in the circum-Mediterranean area: Mt. Karacadağ, SE Turkey: European Journal of Mineralogy, v. 22, no. 3, p. 343–362, https://doi.org/10.1127/0935-1221/2010/0022-2024.

Lustrino, M., Keskin, M., Mattioli, M., and Kavak, O., 2012, Heterogeneous mantle sources feeding the volcanic activity of Mt. Karacadağ (SE Turkey): Journal of Asian Earth Sciences, v. 46, p. 120–139, https://doi.org/10.1016/j.jseaes.2011.11.016.

McGee, L.E., and Smith, I.E., 2016, Interpreting chemical compositions of small scale basaltic systems: A review: Journal of Volcanology and Geothermal Research, v. 325, p. 45–60, https://doi.org/10.1016/j.jvolgeores.2016.06.007.

McGee, L.E., Smith, I.E., Millet, M.A., Handley, H.K., and Lindsay, J.M., 2013, Asthenospheric control of melting processes in a monogenetic basaltic system: A case study of the Auckland volcanic field, New Zealand: Journal of Petrology, v. 54, no. 10, p. 2125–2153, https://doi.org/10.1093/petrology/egt043.

Mollo, S., Del Gaudio, P., Ventura, G., Iezzi, G., and Scarlato, P., 2010, Dependence of clinopyroxene composition on cooling rate in basaltic magmas: Implications for thermobarometry: Lithos, v. 118, no. 3–4, p. 302–312, https://doi.org/10.1016/j.lithos.2010.05.006.

Morimoto, N., 1988, Nomenclature of pyroxenes: Mineralogy and Petrology, v. 39, no. 1, p. 55–76, https://doi.org/10.1007/BF01226262.

Mutlu, A.K., and Karabulut, H., 2011, Anisotropic Pn tomography of Turkey and adjacent regions: Geophysical Journal International, v. 187, no. 3, p. 1743–1758, https://doi.org/10.1111/j.1365-246X.2011.05235.x.

Németh, K., and Kereszturi, G., 2015, Monogenetic volcanism: Personal views and discussion: International Journal of Earth Sciences, v. 104, no. 8, p. 2131–2146, https://doi.org/10.1007/s00531-015-1243-6.

Németh, K., Martin, U., and Harangi, S., 2001, Miocene phreatomagmatic volcanism at Tihany (Pannonian Basin, Hungary): Journal of Volcanology and Geothermal Research, v. 111, no. 1–4, p. 111–135, https://doi.org/10.1016/S0377-0273(01)00223-2.

Németh, K., Risso, C., Nullo, F., and Kereszturi, G., 2011, The role of collapsing and cone rafting on eruption style changes and final cone morphology: Los Morados scoria cone, Mendoza, Argentina: Central European Journal of Geosciences, v. 3, no. 2, p. 102–118.

Notsu, K., Fujitani, T., Ui, T., Matsuda, J., and Ercan, T., 1995, Geochemical features of collision-related volcanic rocks in Central and Eastern Anatolia, Turkey: Journal of Volcanology and Geothermal Research, v. 64, no. 3–4, p. 171–191, https://doi.org/10.1016/0377-0273(94)00077-T.

Okay, A.I., and Tüysüz, O., 1999, Tethyan sutures of northern Turkey, *in* Durand, B., Jolivet, L., Horváth, F., and Séranne, M., eds., The Mediterranean Basins: Tertiary Extension within the Alpine Orogen: Geological Society, London, Special Publication 156, p. 475–515.

Okay, A.I., Zattin, M., and Cavazza, W., 2010, Apatite fission-track data for the Miocene Arabia-Eurasia collision: Geology, v. 38, no. 1, p. 35–38, https://doi.org/10.1130/G30234.1.

Oyan, V., Keskin, M., Lebedev, V.A., Chugaev, A.V., and Sharkov, E.V., 2016, Magmatic evolution of the early Pliocene Etrüsk stratovolcano, Eastern Anatolian collision zone, Turkey: Lithos, v. 256–257, p. 88–108, https://doi.org/10.1016/j.lithos.2016.03.017.

Özdemir, Y., Blundy, J., and Güleç, N., 2011, The importance of fractional crystallization and magma mixing in controlling chemical differentiation at Süphan stratovolcano, Eastern Anatolia, Turkey: Contributions to Mineralogy and Petrology, v. 162, no. 3, p. 573–597, https://doi.org/10.1007/s00410-011-0613-8.

Özsayın, E., Ciner, T.A., Rojay, F.B., Dirik, R.K., Melnick, D., and Fernandez-Blanco, D., 2013, Plio-Quaternary extensional tectonics of the Central Anatolian Plateau: A case study from the Tuz Gölü Basin, Turkey: Turkish Journal of Earth Sciences, v. 22, no. 5, p. 691–714.

Palme, H., and O'Neill, H.S.C., 2003, Cosmochemical estimates of mantle composition, *in* Carlson, R.W., ed., Treatise on Geochemistry: Volume 2. Mantle and Core: Oxford, UK, Elsevier-Pergamon, p. 1–39.

Pearce, J.A., 1983, Role of the sub-continental lithosphere in magma genesis at active continental margins, *in* Hawkesworth, C.J., and Norry, M.J., eds., Continental Basalts and Mantle Xenoliths: Nantwich, UK, Shiva, p. 230–249.

Pearce, J.A., 2008, Geochemical fingerprinting of oceanic basalts with applications to ophiolite classification and the search for Archean oceanic crust: Lithos, v. 100, no. 1–4, p. 14–48, https://doi.org/10.1016/j.lithos.2007.06.016.

Pearce, J.A., and Norry, M.J., 1979, Petrogenetic implications of Ti, Zr, Y, and Nb variations in volcanic rocks: Contributions to Mineralogy and Petrology, v. 69, no. 1, p. 33–47, https://doi.org/10.1007/BF00375192.

Pearce, J.A., Bender, J.F., De Long, S.E., Kidd, W.S.F., Low, P.J., Güner, Y., Şaroglu, F., and Mitchell, J.G., 1990, Genesis of collision volcanism in Eastern Anatolia, Turkey: Journal of Volcanology and Geothermal Research, v. 44, no. 1–2, p. 189–229, https://doi.org/10.1016/0377-0273(90)90018-B.

Pfänder, J.A., Münker, C., Stracke, A., and Mezger, K., 2007, Nb/Ta and Zr/Hf in ocean island basalts—Implications for crust-mantle differentiation and the fate of niobium: Earth and Planetary Science Letters, v. 254, no. 1–2, p. 158–172, https://doi.org/10.1016/j.epsl.2006.11.027.

Pfänder, J.A., Jung, S., Münker, C., Stracke, A., and Mezger, K., 2012, A possible high Nb/Ta reservoir in the continental lithospheric mantle and consequences on the global Nb budget—Evidence from continental basalts from central Germany: Geochimica et Cosmochimica Acta, v. 77, p. 232–251, https://doi.org/10.1016/j.gca.2011.11.017.

Pilet, S., 2015, Generation of low-silica alkaline lavas: Petrological constraints, models, and thermal implications, *in* Foulger, G.R., Lustrino, M., and King, S.D., eds., The Interdisciplinary Earth: A Volume in Honor of Don L. Anderson: Geological Society of America Special Paper 514, p. 281–304, https://doi.org/10.1130/2015.2514(17).

Platzman, E.S., Tapirdamaz, C., and Sanver, M., 1998, Neogene anticlockwise rotation of Central Anatolia (Turkey): Preliminary palaeomagnetic and geochronological results: Tectonophysics, v. 299, no. 1–3, p. 175–189, https://doi.org/10.1016/S0040-1951(98)00204-2.

Putirka, K., 2008, Thermometers and barometers for volcanic systems, *in* Putirka, K., and Tepley, F., eds., Minerals, Inclusions and Volcanic Processes: Mineralogical Society of America Reviews in Mineralogy and Geochemistry, v. 69, p. 61–120.

Putirka, K.D., Perfit, M., Ryerson, F.J., and Jackson, M.G., 2007, Ambient and excess mantle temperatures, olivine thermometry, and active vs. passive upwelling: Chemical Geology, v. 241, no. 3–4, p. 177–206, https://doi.org/10.1016/j.chemgeo.2007.01.014.

Rasoazanamparany, C., Widom, E., Valentine, G.A., Smith, E.I., Cortés, J.A., Kuentz, D., and Johnsen, R., 2015, Origin of chemical and isotopic heterogeneity in a mafic, monogenetic volcanic field: A case study of the Lunar Crater volcanic field, Nevada: Chemical Geology, v. 397, p. 76–93, https://doi.org/10.1016/j.chemgeo.2015.01.004.

Reid, M.R., Schleiffarth, W.K., Cosca, M.A., Delph, J.R., Blichert-Toft, J., and Cooper, K.M., 2017, Shallow melting of MORB-like mantle under hot continental lithosphere, Central Anatolia: Geochemistry Geophysics Geosystems, v. 18, no. 5, p. 1866–1888, https://doi.org/10.1002/2016GC006772.

Reilinger, R., McClusky, S., Vernant, P., Lawrence, S., Ergintav, S., Cakmak, R., Özener, H., Kadirov, F., Guliev, İ., Stepanyan, R., Nadariya, M., Hahubia, G., Mahmoud, S., Sakr, K., ArRajehi, A., Paradissis, D., Al-Aydrus, A., Prilepin, M., Guseva, T., Evren, E., Dmitrotsa, A., Filikov, S.V., Gomez, F., Al-Ghazzi, R., and Karam, G., 2006, GPS constraints on continental deformation in the Africa-Arabia-Eurasia continental collision zone and implications for the dynamics of plate interactions: Journal of Geophysical Research–Solid Earth, v. 111, B05411, https://doi.org/10.1029/2005JB004051.

Roeder, P.L., and Emslie, R., 1970, Olivine-liquid equilibrium: Contributions to Mineralogy and Petrology, v. 29, no. 4, p. 275–289, https://doi.org/10.1007/BF00371276.

Rollinson, H.R., 1993, Using Geochemical Data: Evaluation, Interpretation, Presentation: London, Pearson Prentice Hall, 352 p.

Schildgen, T.F., Cosentino, D., Bookhagen, B., Niedermann, S., Yıldırım, C., Echtler, H., Wittmann, H., and Strecker, M.R., 2012, Multi-phased uplift of the southern margin of the Central Anatolian Plateau, Turkey: A record of tectonic and upper mantle processes: Earth and Planetary Science Letters, v. 317–318, p. 85–95, https://doi.org/10.1016/j.epsl.2011.12.003.

Schildgen, T.F., Yıldırım, C., Cosentino, D., and Strecker, M.R., 2014, Linking slab break-off, Hellenic trench retreat, and uplift of the Central and Eastern Anatolian Plateaus: Earth-Science Reviews, v. 128, p. 147–168, https://doi.org/10.1016/j.earscirev.2013.11.006.

Schleiffarth, W.K., Darin, M.H., Reid, M.R., and Umhoefer, P.J., 2018, Dynamics of episodic Late Cretaceous–Cenozoic magmatism across Central to Eastern Anatolia—New insights from a comprehensive geochronology compilation: Geosphere, v. 14, no. 5, p. 1990–2008, https://doi.org/10.1130/GES01647.1.

Schmitt, A.K., Danišík, M., Evans, N.J., Siebel, W., Kiemele, E., Aydin, F., and Harvey, J.C., 2011, Acigöl rhyolite field, Central Anatolia (part 1): High-resolution dating of eruption episodes and zircon growth rates: Contributions to Mineralogy and Petrology, v. 162, no. 6, p. 1215–1231, https://doi.org/10.1007/s00410-011-0648-x.

Schmitt, A.K., Danišík, M., Aydar, E., Şen, E., Ulusoy, İ., and Lovera, O.M., 2014, Identifying the volcanic eruption depicted in a neolithic painting at Çatalhöyük, Central Anatolia, Turkey: PLoS One, v. 9, e84711, https://doi:10.1371/journal.pone.0084711.

Şen, E., Aydar, E., Gourgaud, A., and Kürkçüoğlu, B., 2002, Initial explosive phases during extrusion of volcanic lava domes: Example from rhyodacitic dome of Dikkartin Dag, Erciyes stratovolcano, Central Anatolia, Turkey: Comptes Rendus Geoscience, v. 334, no. 1, p. 27–33, https://doi.org/10.1016/S1631-0713(02)01698-X.

Şen, E., Kürkcüoğlu, B., Aydar, E., Gourgaud, A., and Vincent, P.M., 2003, Volcanological evolution of Mount Erciyes stratovolcano and origin of the Valibaba Tepe ignimbrite (Central Ana-

tolia, Turkey): Journal of Volcanology and Geothermal Research, v. 125, no. 3–4, p. 225–246, https://doi.org/10.1016/S0377-0273(03)00110-0.
Şenel, M., ed., 2002, 1/500000 scale geological maps of Turkey: Mineral Research & Exploration General Directorate (in Turkish).
Şenel, M., ed., 2005, 1/100000 scale geological maps of Turkey, Aksaray L32 sheet: Mineral Research & Exploration General Directorate (in Turkish).
Shaw, J.E., Baker, J.A., Menzies, M.A., Thirlwall, M.F., and Ibrahim, K.M., 2003, Petrogenesis of the largest intraplate volcanic field on the Arabian plate (Jordan): A mixed lithosphere–asthenosphere source activated by lithospheric extension: Journal of Petrology, v. 44, no. 9, p. 1657–1679, https://doi.org/10.1093/petrology/egg052.
Smith, I.E.M., and Németh, K., 2017, Source to surface model of monogenetic volcanism: A critical review, *in* Németh, K., Carrasco-Núñez, G., Aranda-Gómez, J.J., and Smith, I.E.M., eds., Monogenetic Volcanism: Geological Society, London, Special Publication 446, p. 1–28.
Strong, M., and Wolff, J., 2003, Compositional variations within scoria cones: Geology, v. 31, no. 2, p. 143–146, https://doi.org/10.1130/0091-7613(2003)031<0143:CVWSC>2.0.CO;2.
Sun, S.S., and McDonough, W.S., 1989, Chemical and isotopic systematics of oceanic basalts: Implications for mantle composition and processes, *in* Saunders, A.D., and Norry, M.J., eds., Magmatism in the Ocean Basins: Geological Society, London, Special Publication 42, p. 313–345, https://doi.org/10.1144/GSL.SP.1989.042.01.19.
Temel, A., Gündoğdu, M.N., and Gourgaud, A., 1998, Petrological and geochemical characteristics of Cenozoic high-K calc-alkaline volcanism in Konya, Central Anatolia, Turkey: Journal of Volcanology and Geothermal Research, v. 85, no. 1–4, p. 327–354, https://doi.org/10.1016/S0377-0273(98)00062-6.
Thompson, R.N., 1984, Dispatches from the basalt front. I. Experiments: Proceedings of the Geologists' Association, v. 95, no. 3, p. 249–262.
Thornton, C.P., and Tuttle, O.F., 1960, Chemistry of igneous rocks: Part 1. Differentiation index: American Journal of Science, v. 258, no. 9, p. 664–684, https://doi.org/10.2475/ajs.258.9.664.
Tokçaer, M., Agostini, S., and Savaşçın, M.Y., 2005, Geotectonic setting and origin of the youngest Kula volcanics (Western Anatolia), with a new emplacement model: Turkish Journal of Earth Sciences, v. 14, no. 2, p. 143–166.
Toprak, V., 1998, Vent distribution and its relation to regional tectonics, Cappadocian volcanics, Turkey: Journal of Volcanology and Geothermal Research, v. 85, no. 1–4, p. 55–67, https://doi.org/10.1016/S0377-0273(98)00049-3.
Türkecan, A., Kuzucuoğlu, C., Mouralis, D., Pastre, J.F., Atıcı, Y., Guillou, H., and Fontugne, M., 2004, Upper Pleistocene Volcanism and Palaeogeography in Cappadocia, Turkey: TÜBİTAK Project No. 101Y109, 180 p.
Ulu, Ü., ed., 2009, 1/100000 scale geological maps of Turkey, Karaman M31 and M32 sheets: Mineral Research & Exploration General Directorate (in Turkish).
Uluocak, E.Ş, Pysklywec, R., and Göğüş, O.H., 2016, Present-day dynamic and residual topography in Central Anatolia: Geophysical Journal International, v. 206, no. 3, p. 1515–1525, https://doi.org/10.1093/gji/ggw225.
Uslular, G., 2016, Petrography and Geochemistry of the Monogenetic Volcanoes in the Southern Part of the Central Anatolian Volcanic Province [M.Sc. thesis]: Menteşe/Muğla, Turkey, Muğla Sıtkı Koçman University, 157 p.
Uslular, G., Gençalioğlu-Kuşcu, G., and Arcasoy, A., 2015, Size-distribution of scoria cones within the Eğrikuyu monogenetic field (Central Anatolia, Turkey): Journal of Volcanology and Geothermal Research, v. 301, p. 56–65, https://doi.org/10.1016/j.jvolgeores.2015.05.006.
Valentine, G.A., and Gregg, T.K.P., 2008, Continental basaltic volcanoes—Processes and problems: Journal of Volcanology and Geothermal Research, v. 177, no. 4, p. 857–873, https://doi.org/10.1016/j.jvolgeores.2008.01.050.
Varol, E., Temel, A., Yürür, T., Gourgaud, A., and Bellon, H., 2014, Petrogenesis of the Neogene bimodal magmatism of the Galatean volcanic province, Central Anatolia, Turkey: Journal of Volcanology and Geothermal Research, v. 280, p. 14–29, https://doi.org/10.1016/j.jvolgeores.2014.04.014.
Whitney, D.L., and Evans, B.W., 2010, Abbreviations for names of rock-forming minerals: The American Mineralogist, v. 95, no. 1, p. 185–187, https://doi.org/10.2138/am.2010.3371.
Wilson, M., Tankut, A., and Güleç, N., 1997, Tertiary volcanism of the Galatia Province, north-west Central Anatolia, Turkey: Lithos, v. 42, no. 1–2, p. 105–121, https://doi.org/10.1016/S0024-4937(97)00039-X.
Wood, C.A., 1980, Morphometric evolution of cinder cones: Journal of Volcanology and Geothermal Research, v. 7, no. 3–4, p. 387–413, https://doi.org/10.1016/0377-0273(80)90040-2.
Workman, R.K., and Hart, S.R., 2005, Major and trace element composition of the depleted MORB mantle (DMM): Earth and Planetary Science Letters, v. 231, no. 1–2, p. 53–72, https://doi.org/10.1016/j.epsl.2004.12.005.
Zindler, A., and Hart, S., 1986, Chemical geodynamics: Annual Review of Earth and Planetary Sciences, v. 14, no. 1, p. 493–571, https://doi.org/10.1146/annurev.ea.14.050186.002425.